SANDIA REPORT

SAND2004-6721
Unlimited Release
Printed March 2005

Final Report to NASAJSC

Thermal Abuse Performance of MOLI, Panasonic and Sanyo 18650 Li-Ion Cells

E. Peter Roth

Prepared by Sandia National Laboratories
Albuquerque, New Mexico 87185 and Livermore, California 94550

Sandia is a multiprogram laboratory operated by Sandia Corporation,
a Lockheed Martin Company, for the United States Department of Energy's
National Nuclear Security Administration under Contract DE-AC04-94AL85000.

Issued by Sandia National Laboratories, operated for the United States Department of Energy by Sandia Corporation.

Available to DOE and DOE contractors from
U.S. Department of Energy
Office of Scientific and Technical Information
P.O. Box 62
Oak Ridge, TN 37831

Telephone: (865)576-8401
Facsimile: (865)576-5728
E-Mail: reports@adonis.osti.gov
Online ordering: http://www.osti.gov/bridge

Available to the public from
U.S. Department of Commerce
National Technical Information Service
5285 Port Royal Rd
Springfield, VA 22161

Telephone: (800)553-6847
Facsimile: (703)605-6900
E-Mail: orders@ntis.fedworld.gov
Online order: http://www.ntis.gov/help/ordermethods.asp?loc=7-4-0#online

SAND2004-6721
Unlimited Release
Printed March 2005

Final Report to NASA JSC

Thermal Abuse Performance of MOLI, Panasonic and Sanyo 18650 Li-Ion Cells

E. Peter Roth
Lithium Research and Development Department
Sandia National Laboratories
P.O. Box 5800
Albuquerque, NM 87185-0613

Abstract

Thermal property measurements of 18650 cells for the Space Shuttle Orbiter Advanced Hydraulic Power System (AHPS, formerly known as EAPU) have been performed. Cells were measured from three commercial manufacturers: E-One MOLI (12 cells), Panasonic (5 cells) and Sanyo (5 cells). Thermal property measurements of the MOLI 18650 cells included measurements of specific heat, self discharge (microcalorimetry), overcharge response and thermal runaway by accelerating rate calorimetry (ARC). The Panasonic and Sanyo cells were measured only for thermal runaway response in the ARC at increasing states of charge (3.8V, 4.0V, 4.2V, 4.3V).

ACKNOWLEDGEMENTS

The author wished to thank David Johnson for his invaluable assistance in performing this work.

Table of Contents

FIGURES

TABLES

ACRONYMS AND ABBREVIATIONS

AHPS	Advanced Hydraulic Power System
ARC	Accelerating Rate Calorimeter/Calorimetry
CID	Current Interrupt Device
EAPU	Electrical Auxiliary Power Unit
SOC	State of Charge

1.0 INTRODUCTION

1.1 Statement of work

The objective of this program is to obtain thermal data to evaluate commercial 18650 Li-ion cells for possible use in the NASA Advanced Hydraulic Power System (AHPS) upgrade to the Space Shuttle Orbiter. Evaluation of these cells includes:

- Acceptance/Electrical Testing
- Heat Capacity (3 cells at 100%SOC)
- ARC Thermal Runaway (3.8V, 4.0V, 4.2V, 4.3V).
- Self Discharge by Microcalorimetry (3.8V, 4.0V, 4.2V) (25°C, 35°C, 50°C, 65°C, 80°C)
- Overcharge heat output (C/2, C/5)

Cells were measured from three commercial manufacturers: E-One MOLI (2.3 Ah), Panasonic (2.1 Ah) and Sanyo (2.1 Ah). A full thermal property characterization was performed on the E-one MOLI cells while the Panasonic and Sanyo cells were measured only for thermal runaway response.

2.0 E-One MOLI Cells

2.1 Electrical Acceptance Tests

Incoming inspection included measurement of open circuit voltage (OCV), weight and dimensions. Table I lists the measured values for the 12 cells received. A load check was performed with a 2.25 A current for 30 seconds to determine load voltage and impedance. The load checks for the Moli cells were performed at the as-received OCV of 3.8V. Figure 1 shows a typical load profile while Table 2 lists the measured load voltages and computed impedances. Two charge/discharge cycles were also performed at a 0.5 A charge rate to 4.2V and a 0.5 A discharge rate to 2.7V. A typical discharge curve is shown in Figure 2 while the discharge capacities are listed in Table 2. All cells were closely matched.

Table 1. Incoming inspection values for MOLI cells.

NASA Moli cells				
#	**Weight(g)**	**Height (mm)**	**Diameter(mm)**	**OCV**
NM01	47.61	65.0	18.1	3.802
NM02	47.53	65.1	18.0	3.802
NM03	47.64	65.0	18.1	3.802
NM04	47.63	65.1	18.0	3.803
NM05	47.60	65.1	18.1	3.803
NM06	47.53	65.1	18.1	3.803
NM07	47.63	65.1	18.1	3.803
NM08	47.56	65.1	18.2	3.802
NM09	47.55	65.0	18.1	3.803
NM10	47.70	65.1	18.1	3.803
NM11	47.57	65.0	18.2	3.802
NM12	47.65	65.1	18.2	3.802
Average	**47.60**	**65.1**	**18.1**	**3.803**
StDev	0.053	0.049	0.067	0.001

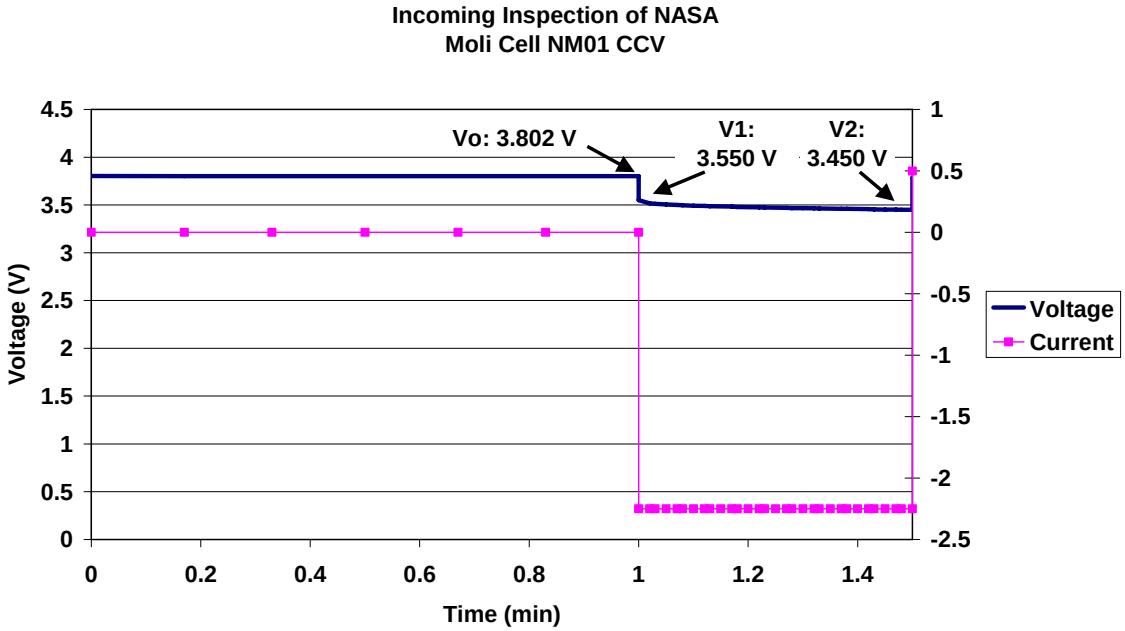

Figure 1. Typical load profile.

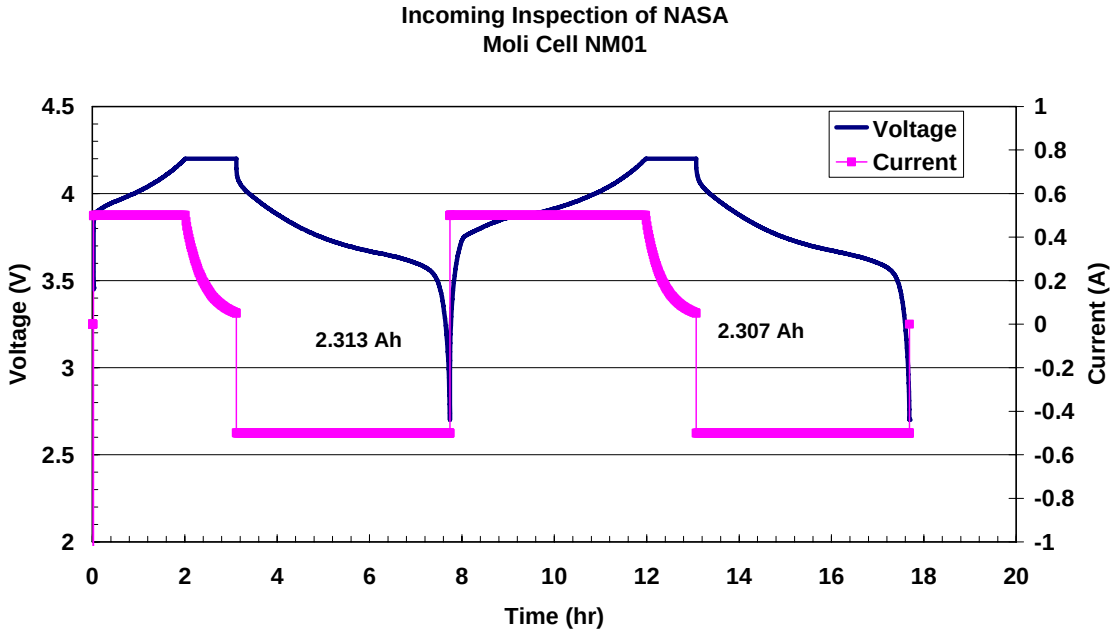

Figure 2. Typical charge/discharge profile.

Table 2. Impedance and discharge capacity values for MOLI cells.

Cell	Discharge Capacity1 (Ah)	Discharge Capacity2 (Ah)	Vo	V1	V2	Ohmic Res. (V0-V1)/I	Final Res. (Vo-V2)/I	Diff.
NM01a	2.313	2.307	3.802	3.550	3.450	0.112	0.156	0.044
NM02a	2.306	2.301	3.802	3.550	3.450	0.112	0.156	0.044
NM03a	2.310	2.305	3.802	3.545	3.445	0.114	0.159	0.044
NM04a	2.315	2.308	3.802	3.523	3.422	0.124	0.169	0.045
NM05a	2.316	2.308	3.802	3.541	3.439	0.116	0.161	0.045
NM06a	2.310	2.303	3.802	3.551	3.448	0.112	0.157	0.046
NM07a	2.306	2.298	3.802	3.484	3.401	0.141	0.178	0.037
NM08a	2.307	2.301	3.802	3.541	3.429	0.116	0.166	0.050
NM09a	2.308	2.302	3.802	3.547	3.447	0.113	0.158	0.044
NM10a	2.319	2.311	3.802	3.545	3.443	0.114	0.160	0.045
NM11a	2.311	2.304	3.802	3.550	3.449	0.112	0.157	0.045
NM12a	2.311	2.304	3.802	3.543	3.441	0.115	0.160	0.045
Avg=	**2.311**	**2.304**			**Avg=**	**0.117**	**0.161**	**0.045**
Std. Dev.=	0.004	0.004			Std. Dev.=	0.008	0.007	0.003

2.2 Heat Capacity Tests

Heat capacity was measured in the Accelerating Rate Calorimeter (ARC) using techniques that we have described previously. Generally, the ARC is in the adiabatic mode while heat is applied to the cell using a resistive wire wrapped around the cell. The slope of the temperature/time profile gives the heat capacity. Prior to cell measurements, heat capacities of known reference materials (Cu, Al) are measured using the same addenda materials. These calibration and addenda values were used for the actual cell heat capacity determinations. Figure 3 shows the ARC temperature profile for 4 heating rates of Moli cell #1. Average heat capacity values are calculated for each cell. It was found that the lower two temperature values gave the most consistent values for heat capacity. Table 3 lists the heat capacity values for the three cells measured. The average specific heat of the three cells is 0.823 J/g-C (1.9 % Std. Dev.) that is slightly lower than the 0.902 J/g-C measured previously for the Sony cells. The major difference results from the 13% higher mass of the Moli cells.

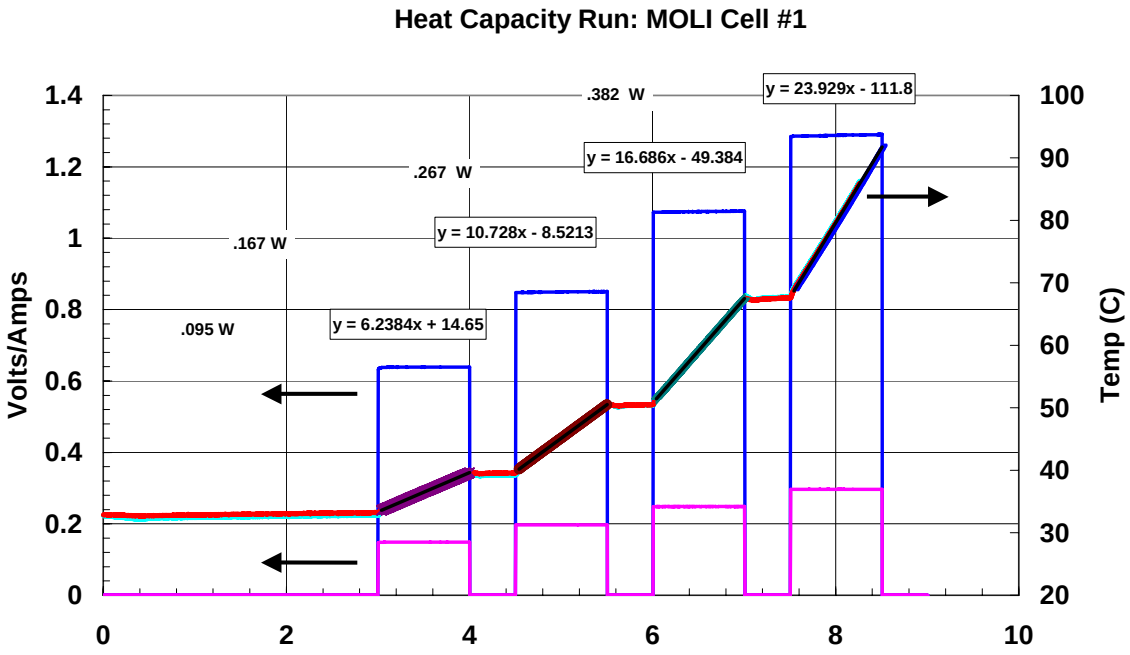

Figure 3. ARC temperature profile for heat capacity measurement.

Table 3. Heat capacity values for three MOLI cells.

Cell #	Average Heat Capacity (J/C)	Specific Heat (J/g-C)
1	38.0	0.806
2	38.8	0.826
3	39.5	0.837
Avg.	**38.8**	**0.823**
Std.Dev.	0.72	0.016
% Std. Dev.	1.9%	1.9%

2.3 Microcalorimetry:

Microcalorimetry was performed on the Moli cells at three cell voltages (3.8V, 4.0V, 4.2V). Measurements were performed at 25°C, 35°C, 45°C, 65°C and 80°C for periods of at least 25 hours. Some cells were measured for longer time periods if the initial measurements overlapped with the weekend. Figure 4 shows the heat outputs at each temperature as a function of increasing cell voltage while Figure 5 shows the heat output at each voltage as a function of increasing temperature. All heat output values were taken over the time period 24-25hrs after the cell was placed in the microcalorimeter as a common reference temperature range. This delay time was necessary to allow the microcalorimeter to fully equilibrate after the temperature disturbance from the inserted cell. These values were used to calculate the activation energy for each cell voltage as shown in Figure 6. Table 4 lists the measured values. The activation energies decreased with increasing cell voltage from 15.6 kcal/mole to 12.2 kcal/mole. The average activation energy was 13.9 kcal/mole (58.0 kJ/mole).

The heat outputs from the cells decreased as a function of time and were seen to obey a power law function as seen previously for the Sony cells. The only cells that did not clearly fit this form were the cells measured at 25°C. The response for these cells was different because there was no clear start time for the self-discharge reaction. The cells were already near this temperature during the cycling and handling prior to insertion into the microcal. Figures 7-11 show the microcalorimeter heat output for each cell voltage as a function of temperature. The functional form of the heat output can be expressed as:

$$\text{Heat Out (uW)} = A \times (\text{time(hrs)})^{B}$$

The “A” term is the prefactor indicating the magnitude of the heat output one hour after being placed in the microcal at the measurement temperature. The “B” term is the power exponent of the time decay. Table 5 lists the values for the fits to each cell at increasing voltage and temperature. The prefactor term increases with increasing voltage and temperature while the power term can be expressed as an average of B= -0.22. Figure 12 shows that the prefactor “A” terms themselves can be fit with a power law curve and can be used to interpolate this prefactor which, along with the average power exponent, can be used to calculate the heat output over this entire temperature range for the three cell voltages measured. The self-discharge reaction is primarily an irreversible reaction that results in greater cell stability with time. These heat outputs represent the initial cell response when first exposed to these voltage and temperature conditions. Subsequent cell response when re-exposed after initial self-discharge reactions will be less than indicated here.

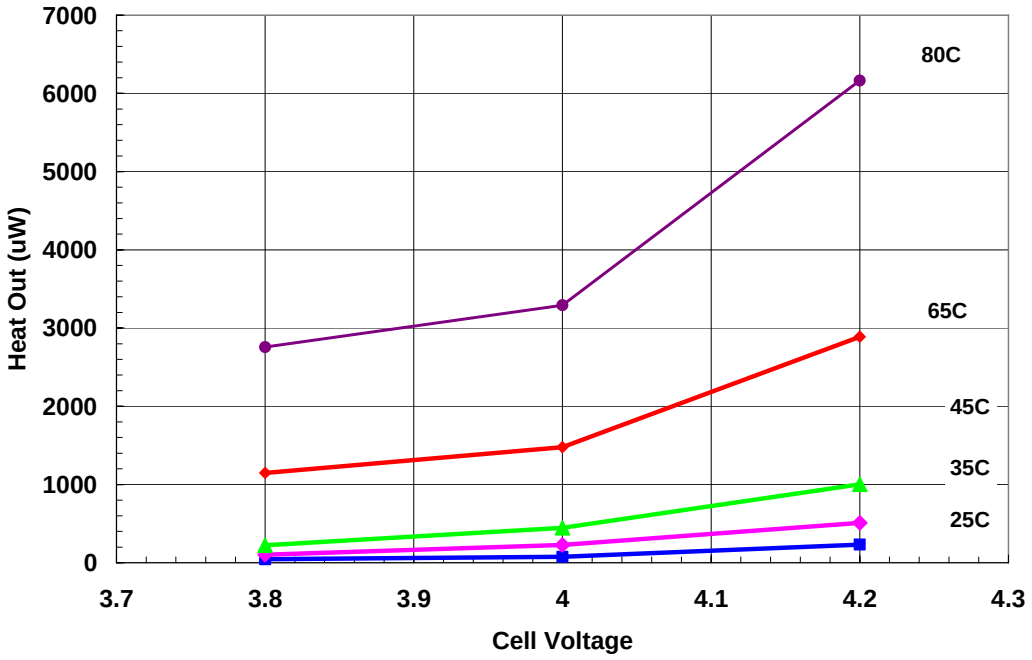

Figure 4. Heat output at increasing temperature as a function of cell voltage.

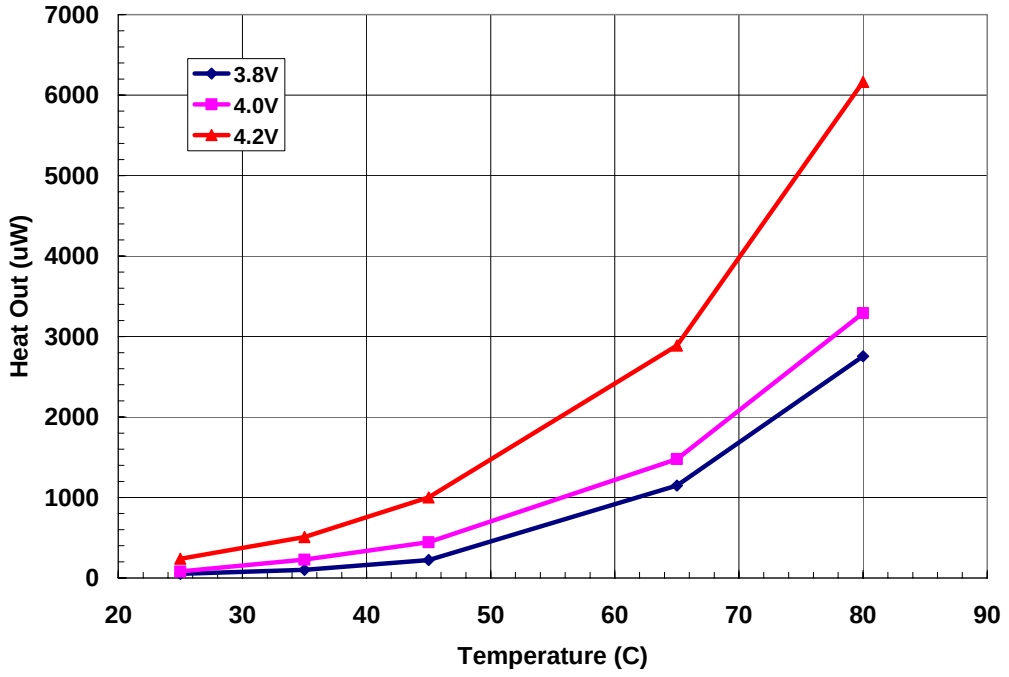

Figure 5. Heat output for each cell voltage as a function of increasing temperature.

Table 4. Heat output and activation energies at increasing SOC and temperature.

Voltage	Temp (C)	Heat Out (uW)	slope	E(Kcal/mole)
3.8V	25	50.1	7862.2	15.62
3.8V	35	101.7		
3.8V	45	223.3		
3.8V	65	1149.3		
3.8V	80	2756.3		
4.0V	25	80.2	6925.7	13.76
4.0V	35	228.4		
4.0V	45	445.3		
4.0V	65	1477		
4.0V	80	3290.7		
4.2V	25	238.5	6152.8	12.23
4.2V	35	509		
4.2V	45	1001.5		
4.2V	65	2889		
4.2V	80	6163.7		
			Avg=	13.87
			std dev=	1.70
			%s.d.=	12.3%

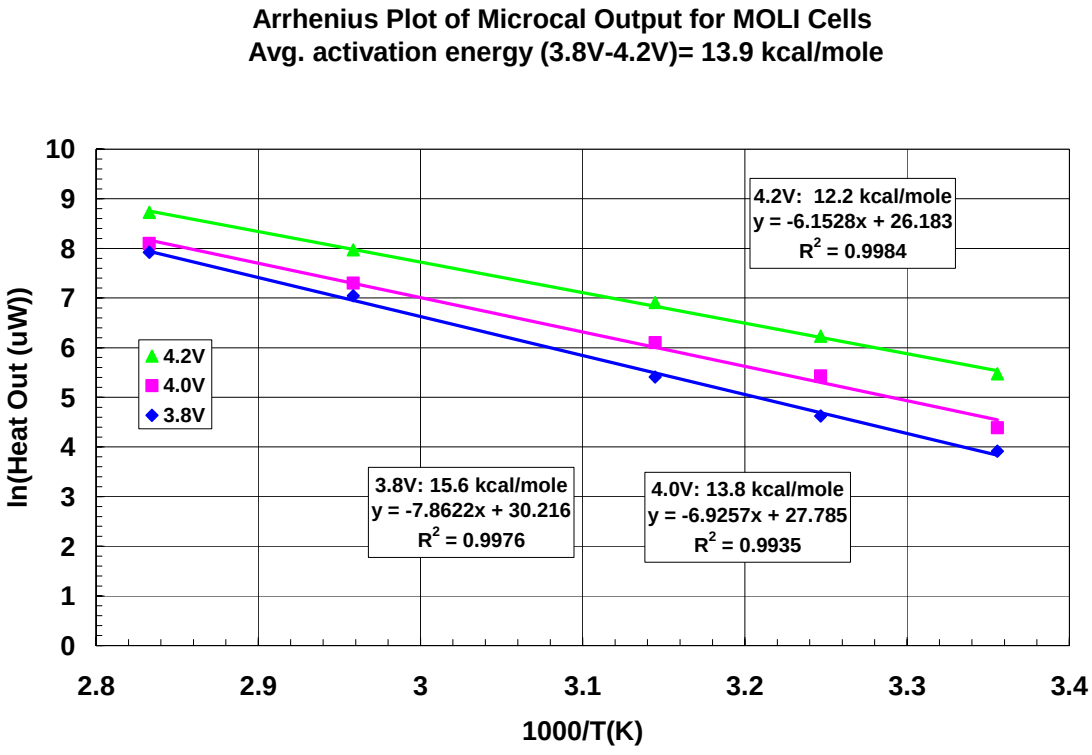

Figure 6. Activation energy plots for cells at increasing SOC.

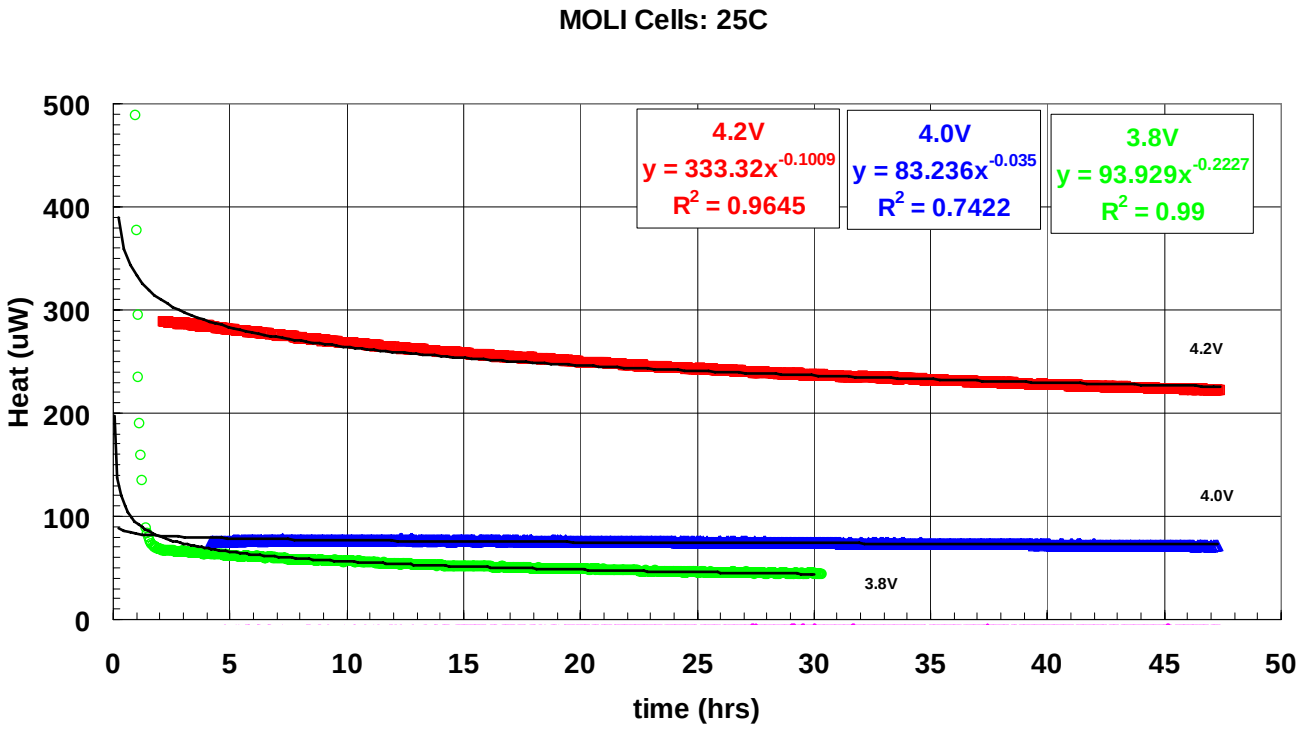

Figure 7. Microcal heat output for cells with increasing voltage at 25°C.

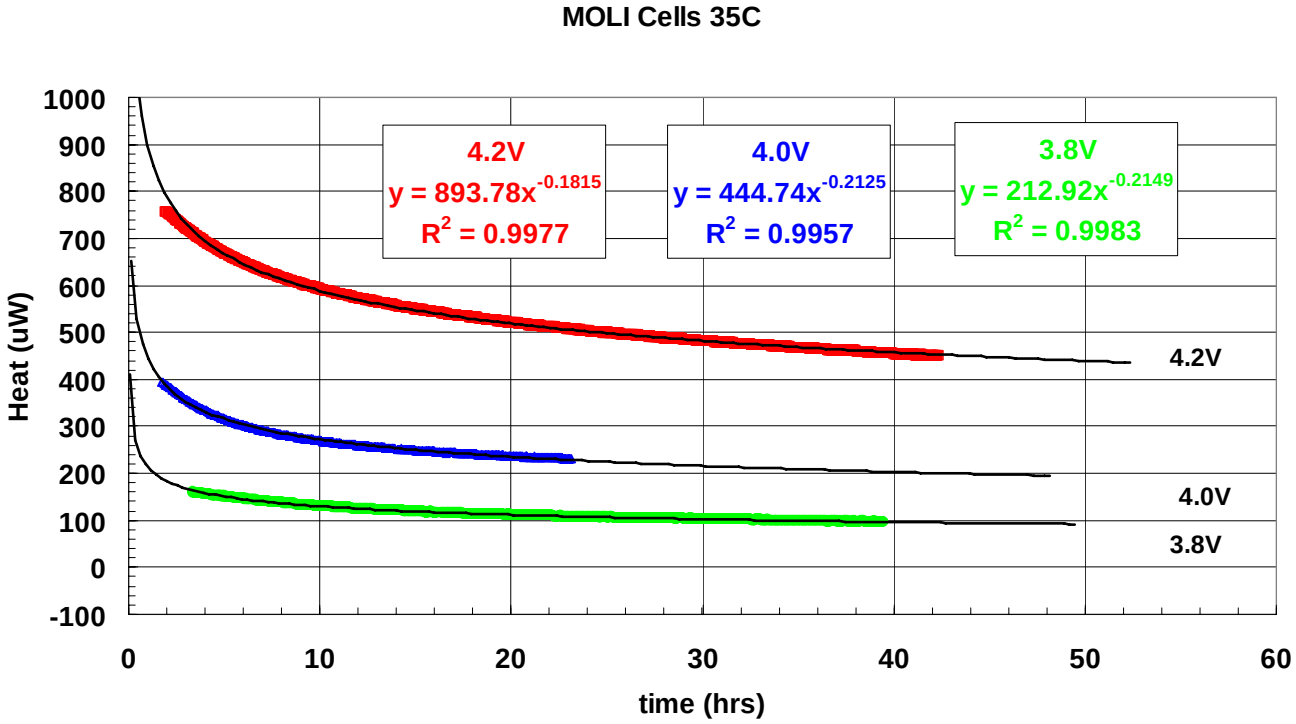

Figure 8. Heat output for cells with increasing voltage at 35°C.

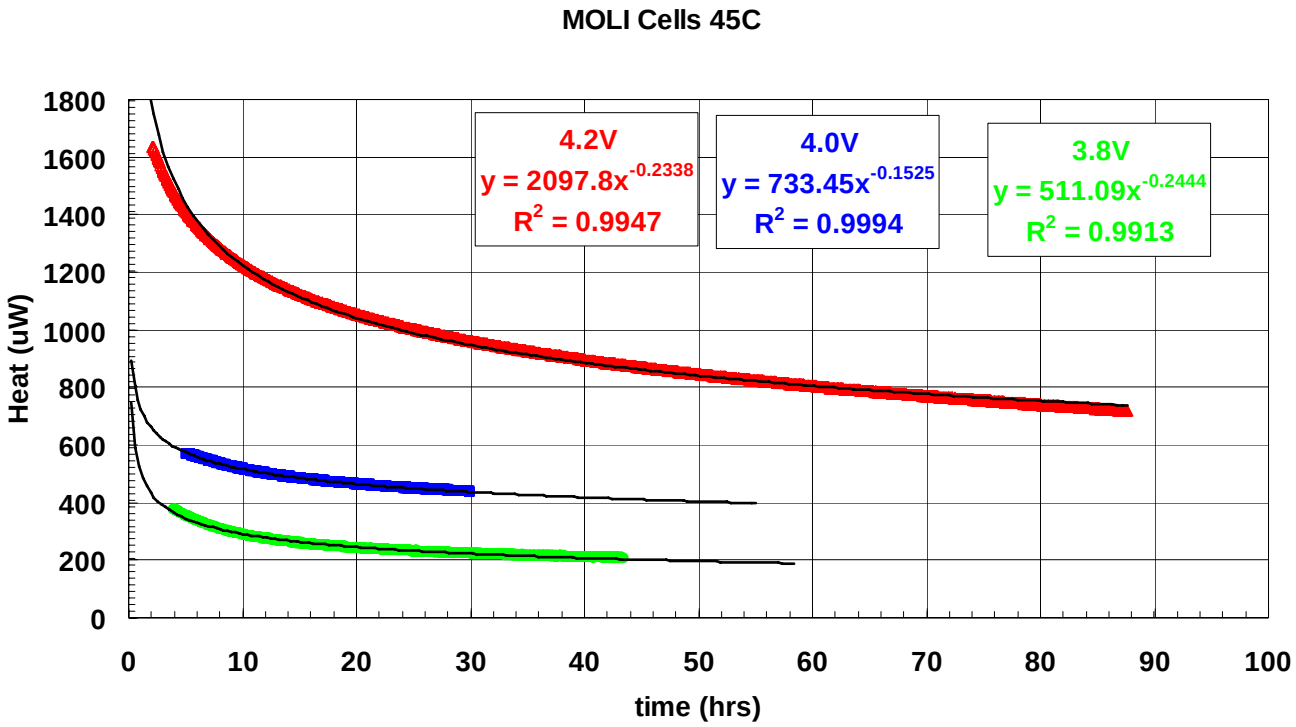

Figure 9. Heat output for cells with increasing voltage at 45°C.

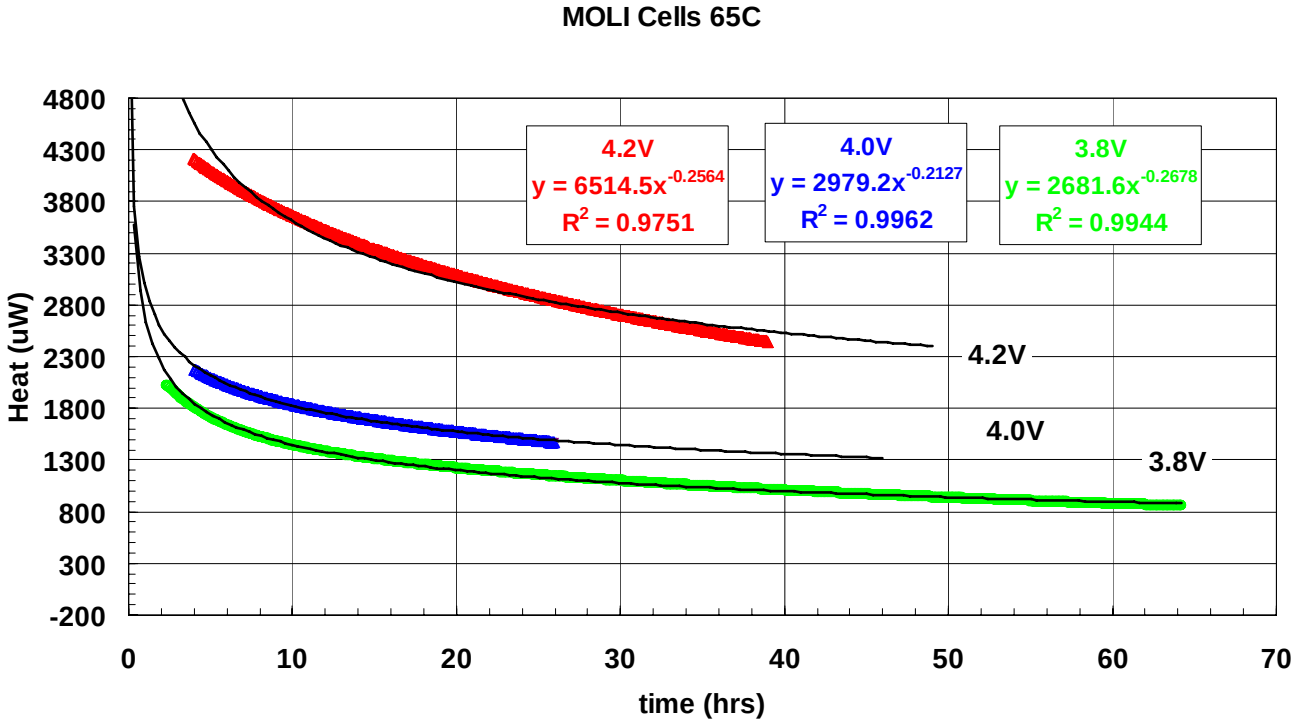

Figure 10. Heat output for cells with increasing voltage at 65°C.

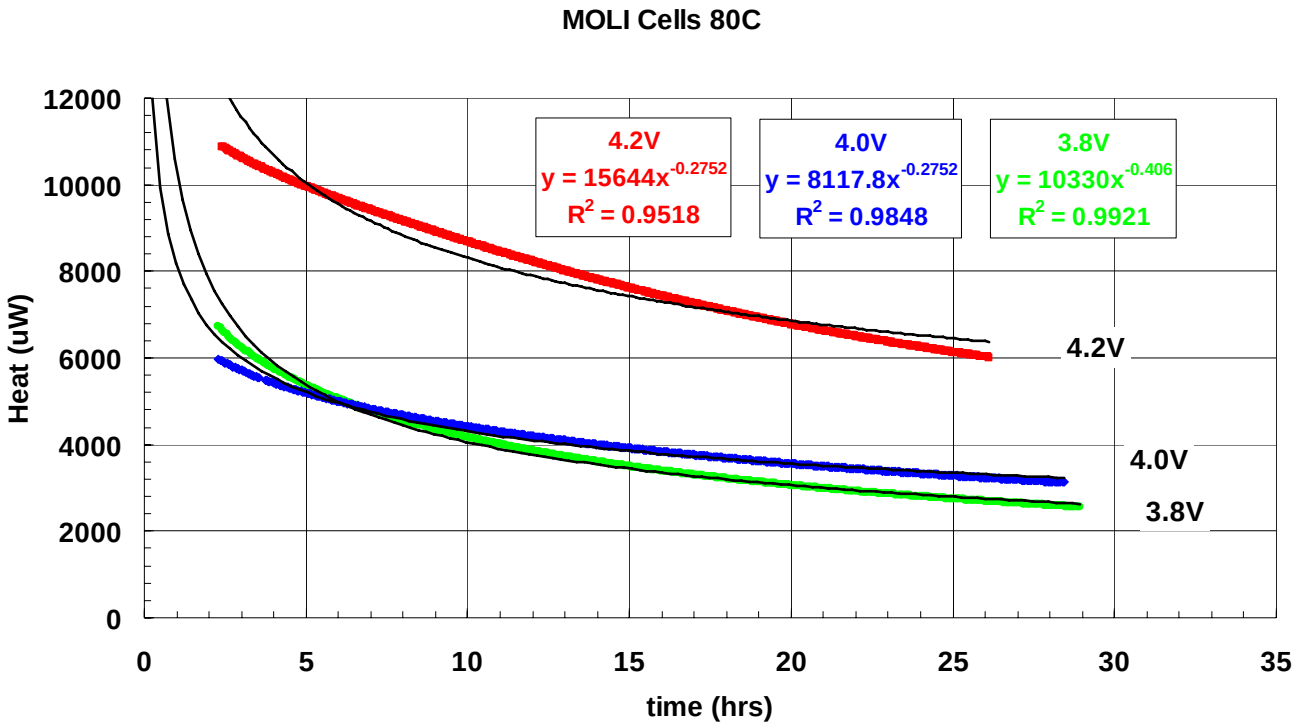

Figure 11. Heat output for cells with increasing voltage at 80°C.

Table 5. Summary of power law functional values fitting the microcalorimeter heat outputs as a function of time (x=time in hrs).

Cell	Temp(C)	Voltage	prefactor "A"	power "B"	Function	
5	25	3.8	93.9	-0.222	y = 93.867x-0.2224	
5	25	4	82.6	-0.028	y = 82.591x-0.0283	
5	25	4.2	336.8	-0.11	y = 336.81x-0.1096	
6	35	3.8	212.9	-0.215	y = 212.92x-0.2149	
6	35	4	444.7	-0.212	y = 444.74x-0.2125	
6	35	4.2	893.8	-0.182	y = 893.78x-0.1815	
7	45	3.8	511.1	-0.244	y = 511.09x-0.2444	
7	45	4	733.5	-0.152	y = 733.45x-0.1525	
7	45	4.2	2098	-0.234	y = 2097.8x-0.2338	
8	65	3.8	2682	-0.268	y = 2681.6x-0.2678	
8	65	4	2979	-0.213	y = 2979.2x-0.2127	
8	65	4.2	6514	-0.256	y = 6514.5x-0.2564	
9	80	3.8	10330	-0.406	y = 10330x-0.406	
9	80	4	8117	-0.275	y = 8117.8x-0.2752	
9	80	4.2	15644	-0.275	y = 15644x-0.2752	
				avg	**std dev**	**%std dev**
			>25C <80C	**-0.220**	**0.036**	**16.6%**

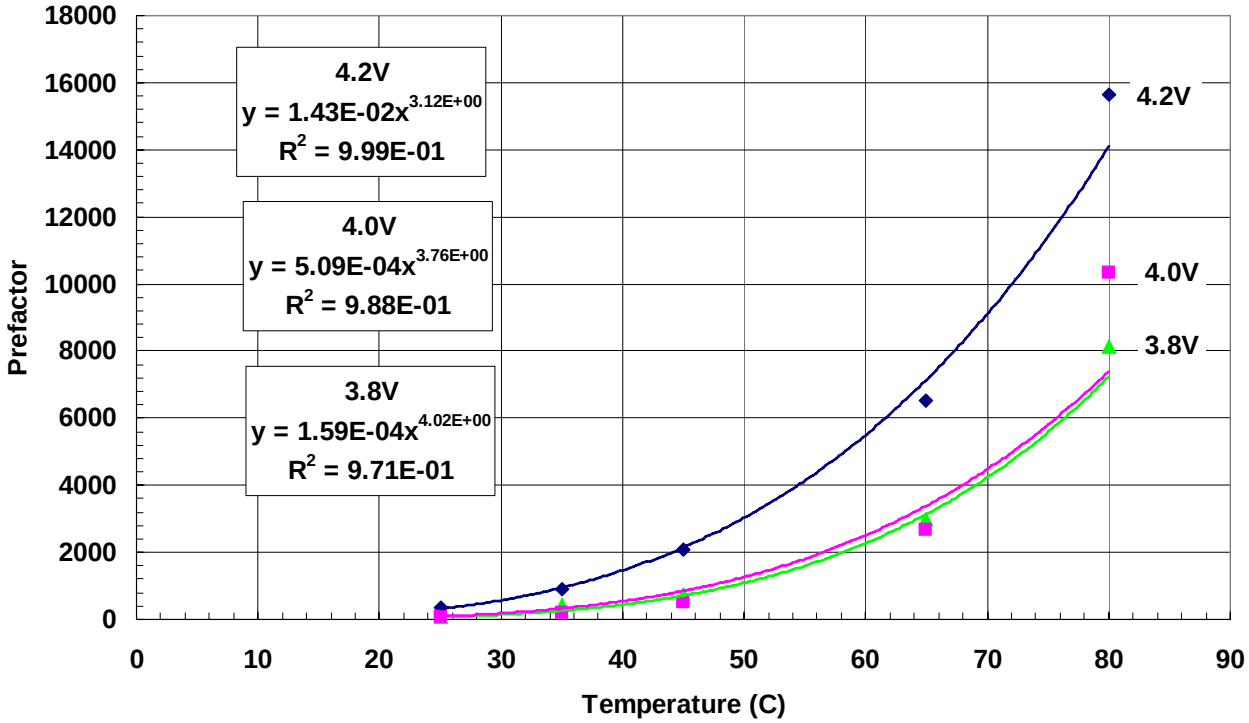

Figure 12. Functional fits to Prefactor "A" terms for self-discharge heat output.

2.4 Overcharge

2.4.1 Overcharge at (C/5)

Quantitative measurements of the heat flow from the cell during overcharge were initially performed at a C/5 (480mA) charge rate starting at 100%SOC (4.2V). A schematic of the test apparatus is shown in Figure 13. The cell was placed in a brass inner cylinder that allows good thermal contact to the cell and smoothes out any temperature variations, allowing a radially symmetric flow of heat. This inner cylinder was thermocoupled and wrapped with layers on insulating glass tape that serves as a fixed thermal resistance. This fixture was then placed in an outer brass cylinder that was thermocoupled to allow measurement of the delta T across the tape in three locations. This system was calibrated with a heated insert with the same dimensions as an 18650 cell. The insert was then removed without disturbing the calibrated heat path through the glass tape. Cells were then inserted and overcharged at the selected rate. The delta T across the tape was used with the calibration function to calculate the heat generated by the cells. The fixture was placed in a Lexan container that was sealed to allow flow through of N_2 gas for real time gas analysis by FTIR, MS and GC.

The current and voltage profiles are shown in Figure 14 while the temperature profile is shown in Figure 15. The cell charged continuously for almost 250 minutes until the current interrupt device (CID) activated and the current dropped to zero. The power supply voltage was limited to 12V at this time. After observing that the cell was cooling and did not appear to be likely to go into a thermal runaway, the power supply voltage was increased to 60V to simulate the higher voltages that might be experienced in a module. The current increased initially due to the increased power surge but then also started to drop. The test was then terminated. Two voltage peaks were observed during the overcharge at 4.95V and 5.05V. At both of these peaks the cell temperature and heat output showed an increase in the rate of rise. These peaks occurred at low cell temperatures of only 25°C and 37°C. Figure 16 shows the cell voltage and the corresponding heat output. The heat output averaged around 22mW prior to these increases. The heat output was increasing rapidly up to the point of the CID activation and reached a value of 1.25 watts. The subsequent increase in applied voltage spiked the heat output to 1.6 watts. Figure 17 shows the heat output and cell voltage plotted as a function of %SOC. The two voltage peaks occurred at 160%SOC and 177%SOC followed by CID activation at 185%SOC. We have seen single voltage peaks at 5.13V in our test cells built with similar chemistry. These lower peaks may result from overcharge additives used by this manufacturer.

During the overcharge run we measured gas evolution from the cell beginning around 146%SOC and at a cell temperature of 23.6°C. We monitored steadily increasing gas generation during the run but at no time did we see evidence of a cell vent. The internal gases generated during overcharge were able to leak around the crimp seals of the cell. Eventually the gas generation rate increased the internal pressure sufficiently to activate the CID even though some gas was being lost. Without this low-rate leak, the CID would have probably have activated sooner. Gas analysis showed that the gases consisted primarily of CO_2, methane and solvent vapors.

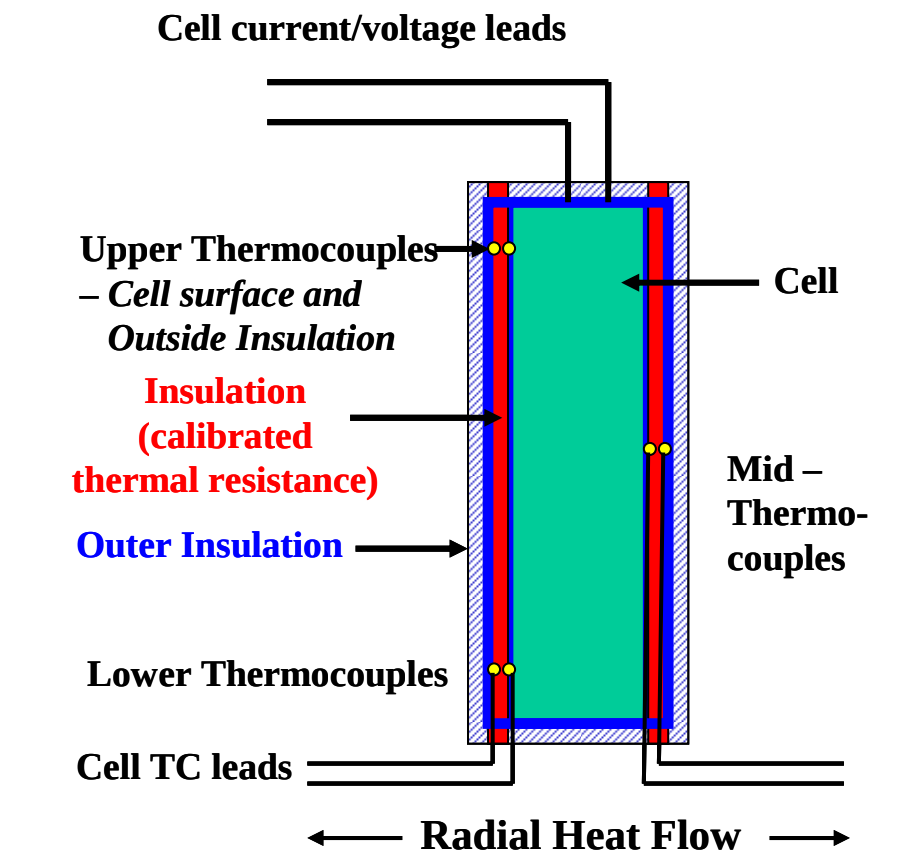

Figure 13. Schematic and photo of overcharge test apparatus.

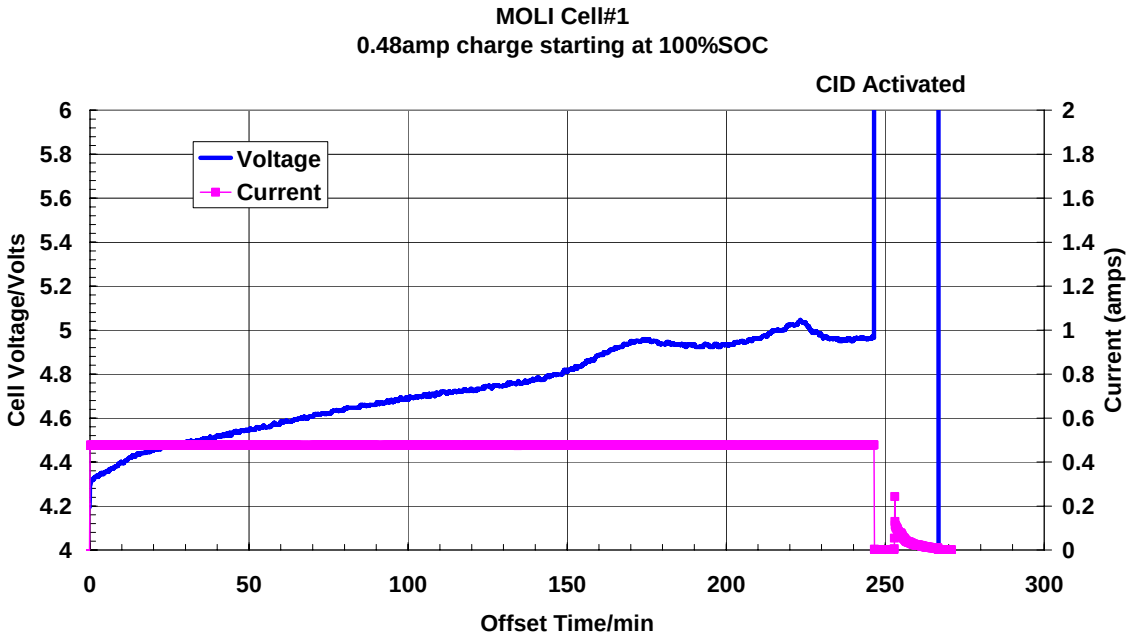

Figure 14. Current and voltage profiles during C/5 overcharge.

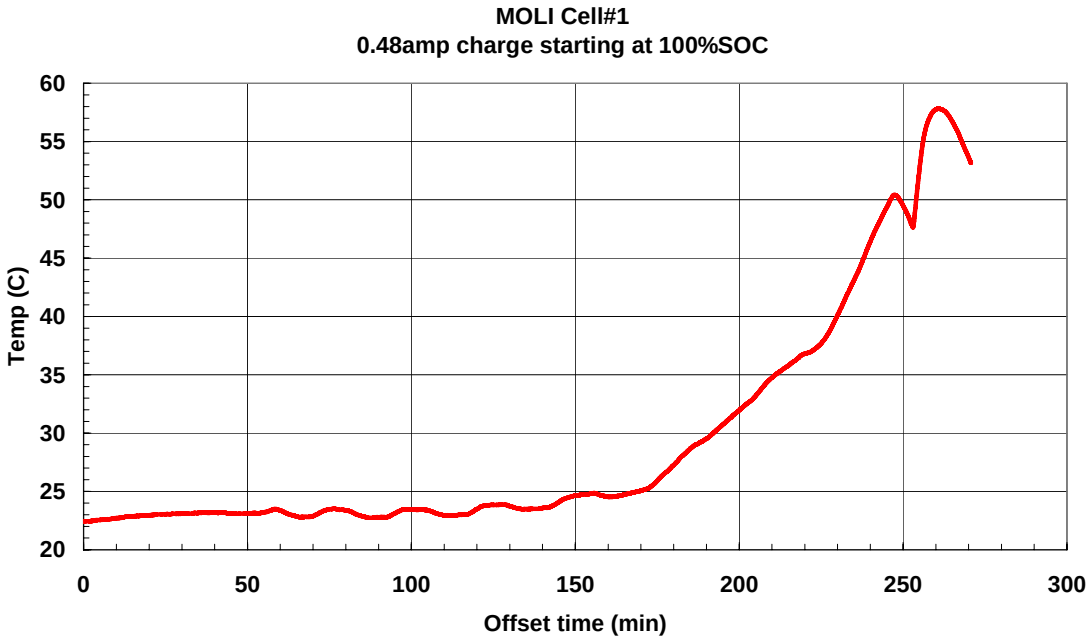

Figure 15. Cell temperature profile during C/5 overcharge.

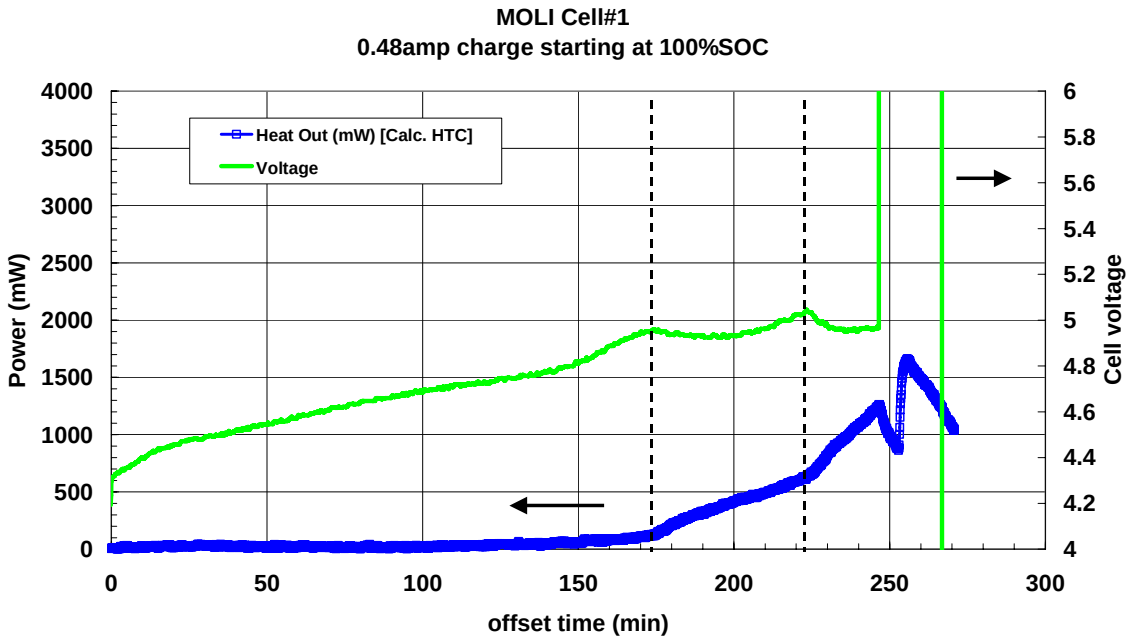

Figure 16. Cell heat output and cell voltage during C/5 overcharge.

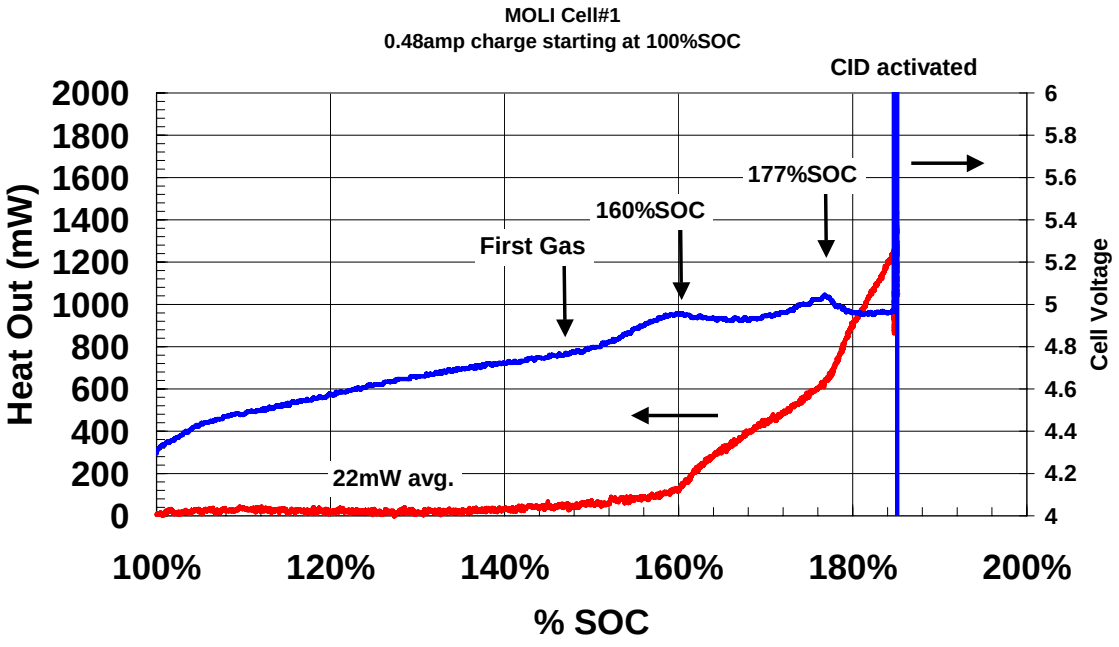

Figure 17. Heat output and cell voltage as a function of %SOC for C/5 charge.

2.4.2 Overcharge at (C/2):

A second overcharge run was performed at a C/2 rate (1.2 A). The current and voltage profiles are shown in Figure 18. The overcharge was started with the cell at 100%SOC and continued until the current interrupt device activated. The voltage profile showed the same two voltage peaks as seen for the C/5 charge. The cell temperature shown in Figure 19 indicates that the cell reached 68°C before the CID activated and then started to cool. No thermal runaway behavior was observed. The corresponding heat output and cell voltage profiles are shown in Figure 20. The first cell voltage peak corresponds to a rapid rise in generated heat. At the second peak, the rate of heat output increased again and peaked at 2600 mW at CID activation. The temperature and heat output were increasing at an accelerating rate at shutdown and could have resulted in a thermal runaway without the CID. The heat output and cell voltage are shown as a function of state of charge in Figure 21. The first voltage occurred at 160%SOC followed by the second peak at 180%SOC. No gas generation was observed during this run.

The average cell temperatures and heat output for the C/5 and C/2 runs are compared in Figures 22 and 23 as a function of SOC. The cell temperature and heat output increased sharply for both charge rates at 160%SOC (first voltage peak) and also at 180%SOC (second voltage peak). The magnitude of the generated heat was greater at the higher charge rate as expected due to increase ohmic and polarization heating. The cell voltage profiles are compared in Figure 24. The two charge rates both resulted in very similar cell voltage responses at a given state of charge. Both cells experienced CID activation at 185%SOC. Since CID activation was limiting the ability to overcharge the cell the third overcharge cell run was not performed.

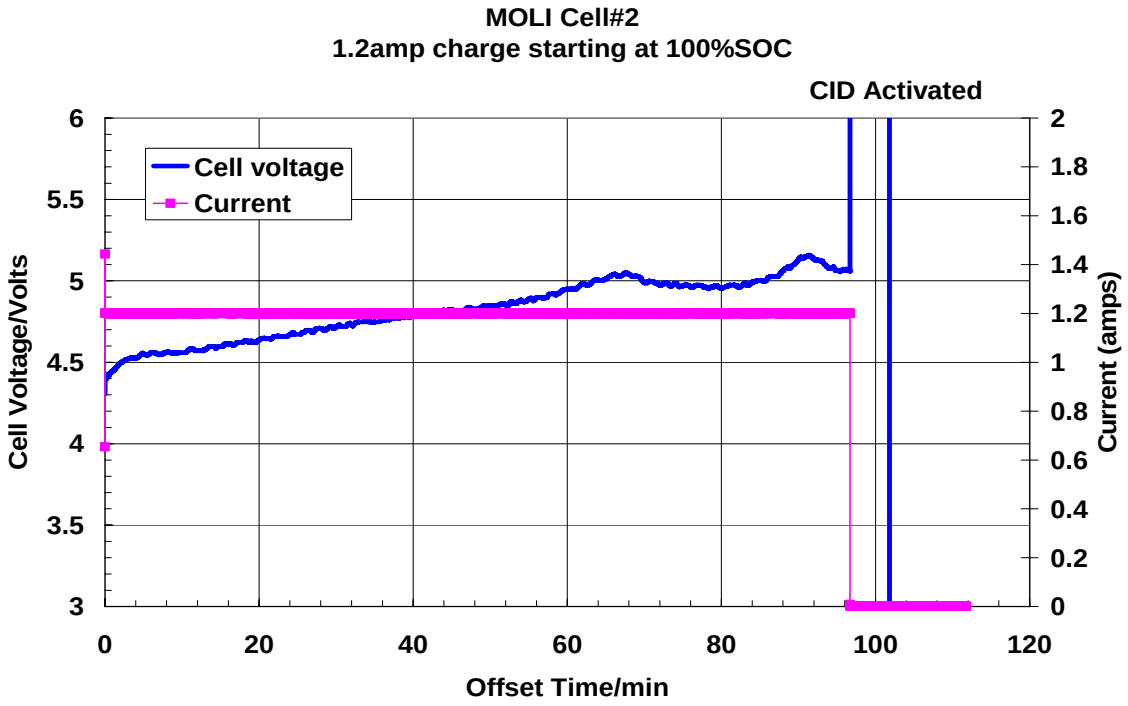

Figure 18. Current and voltage profiles during C/2 overcharge.

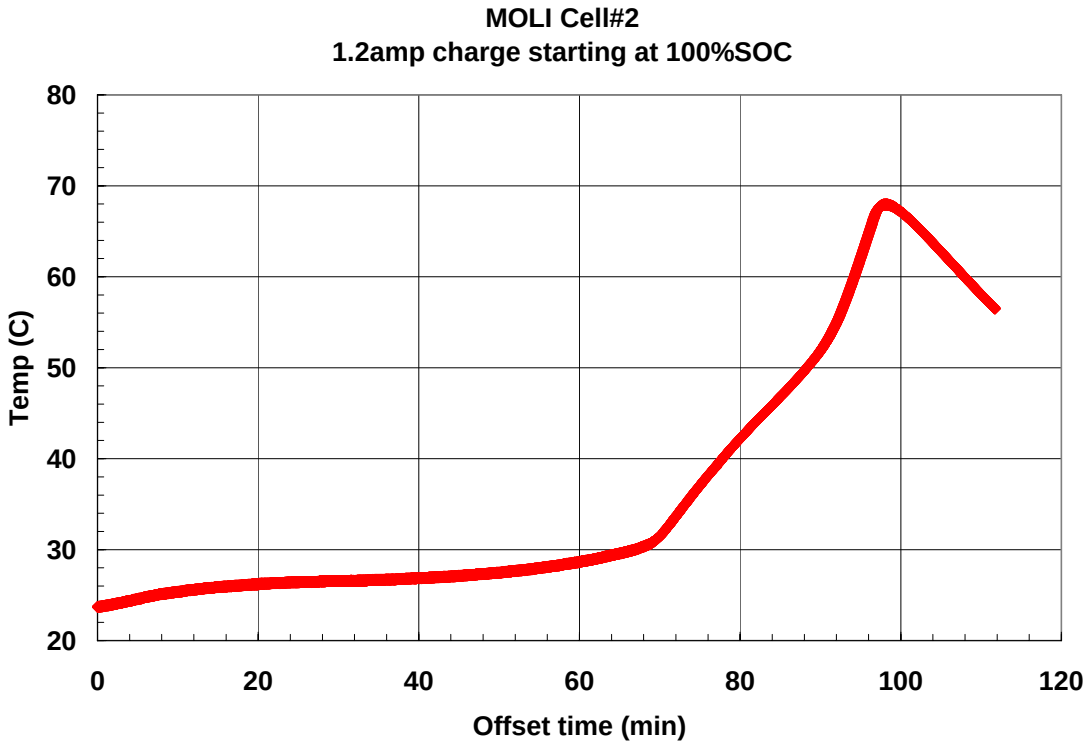

Figure 19. Cell temperature profile during C/2 overcharge.

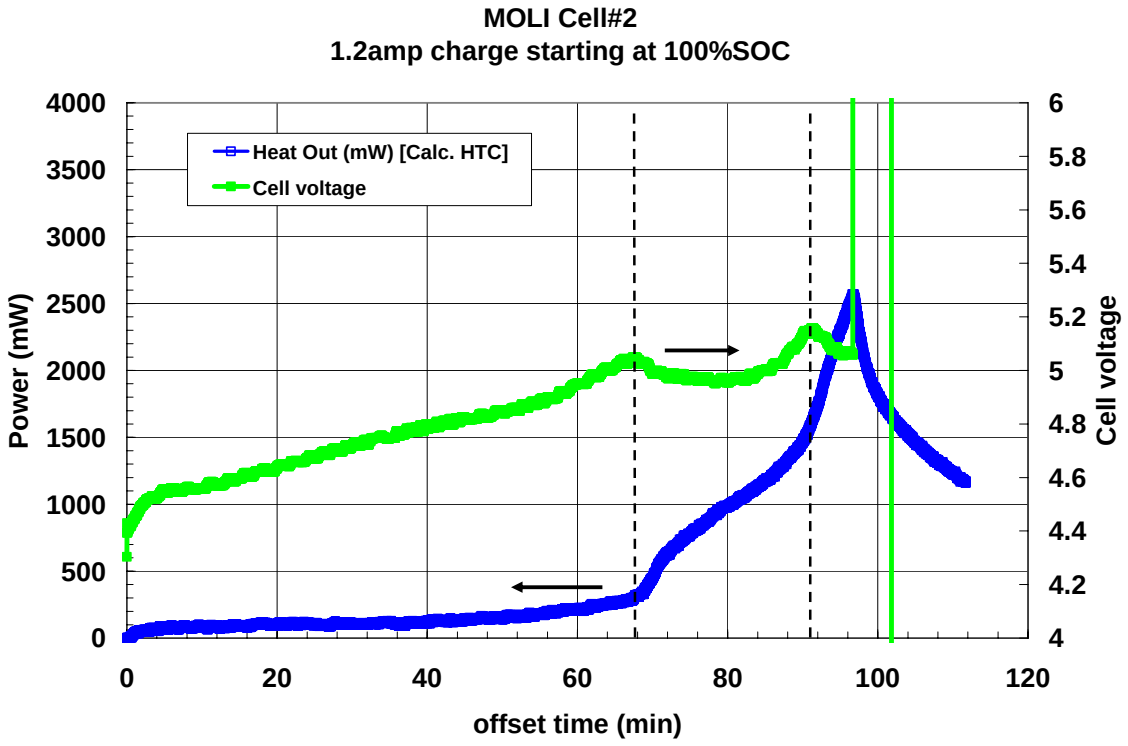

Figure 20. Cell heat output and cell voltage during C/2 overcharge.

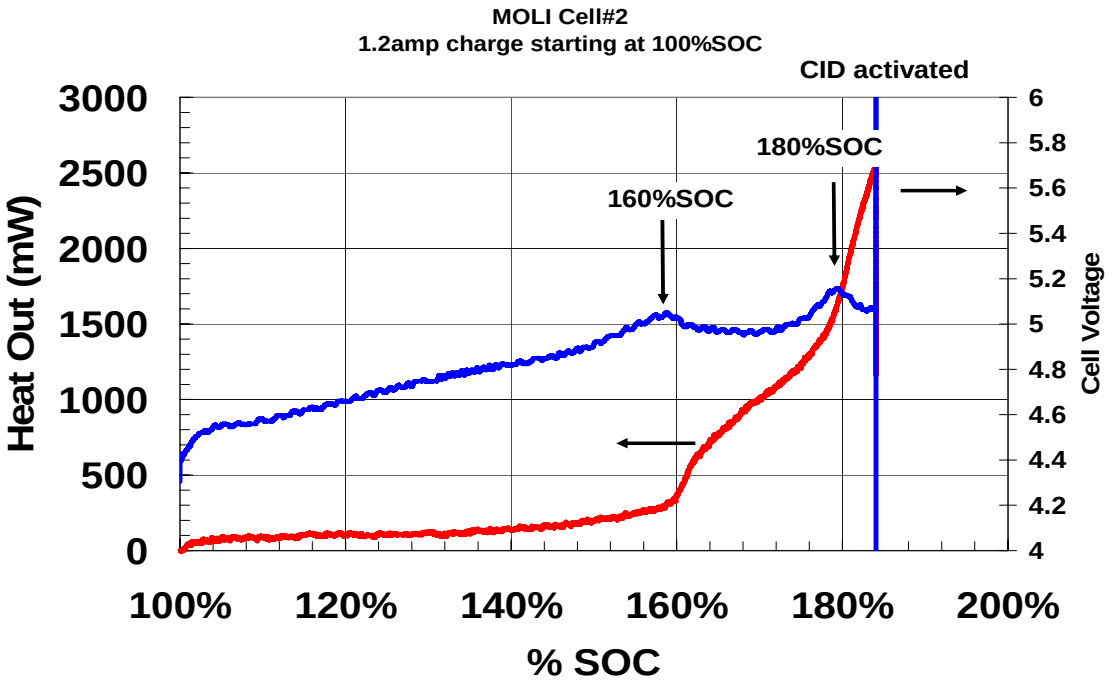

Figure 21. Heat output and cell voltage as a function of %SOC for C/2 charge.

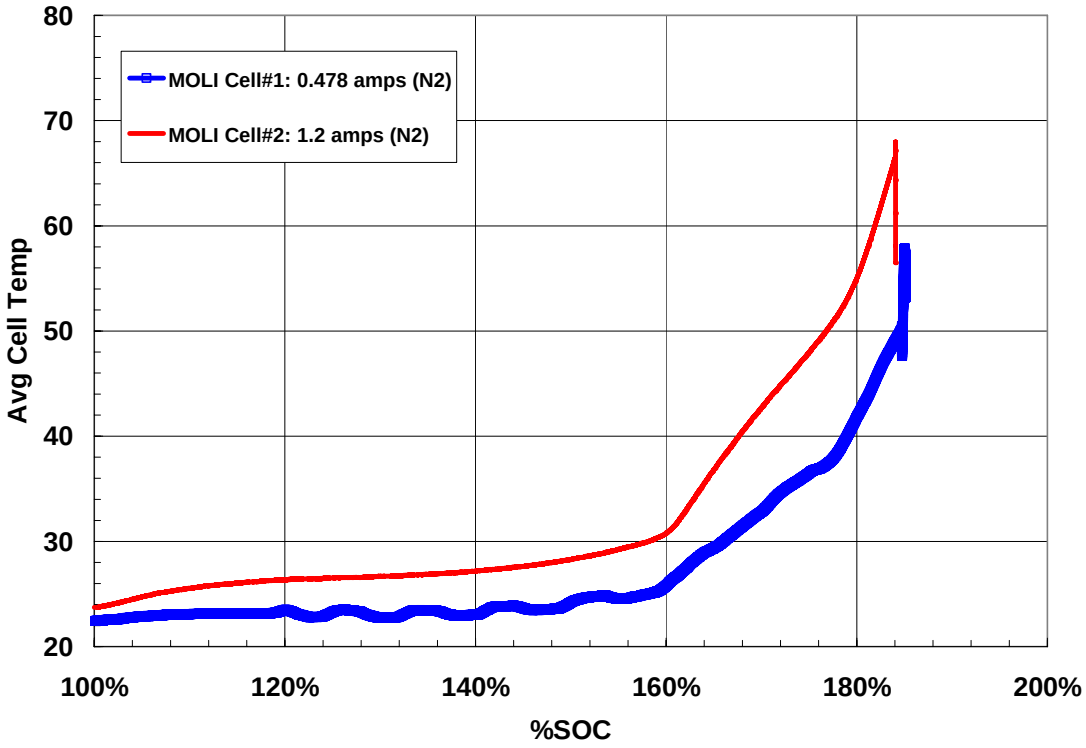

Figure 22. Average cell temperatures of Moli cells during overcharge at C/5 and C/2 charge rates.

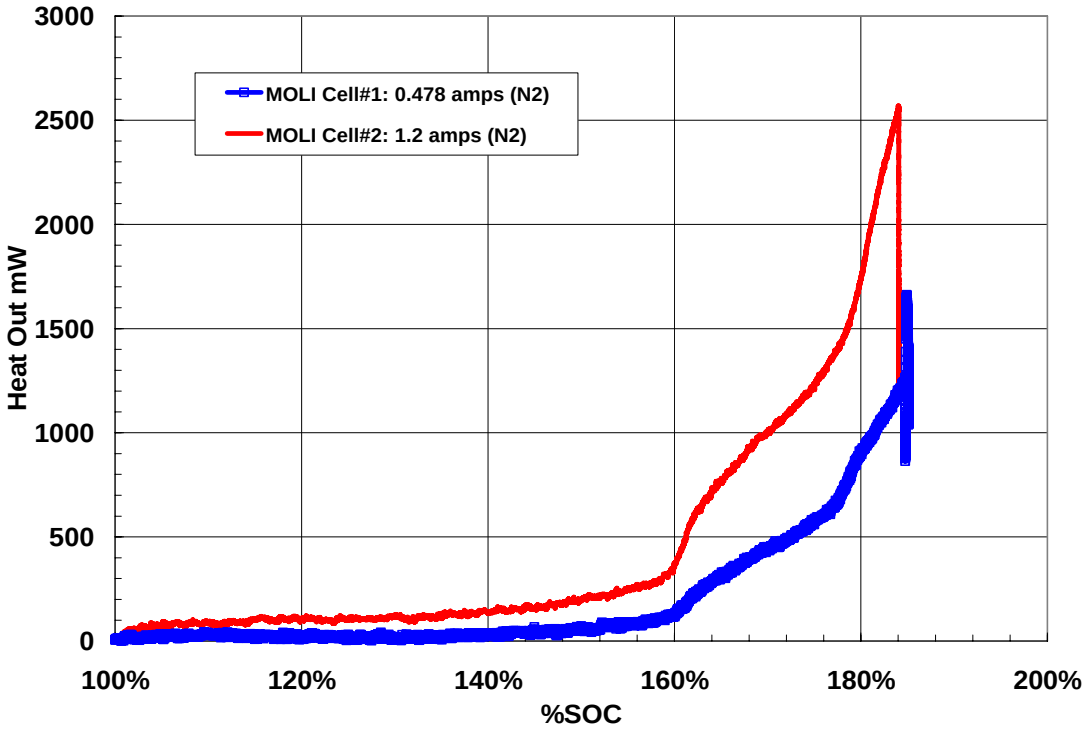

Figure 23. Heat output during overcharge of Moli cells at C/5 and C/2 charge rates.

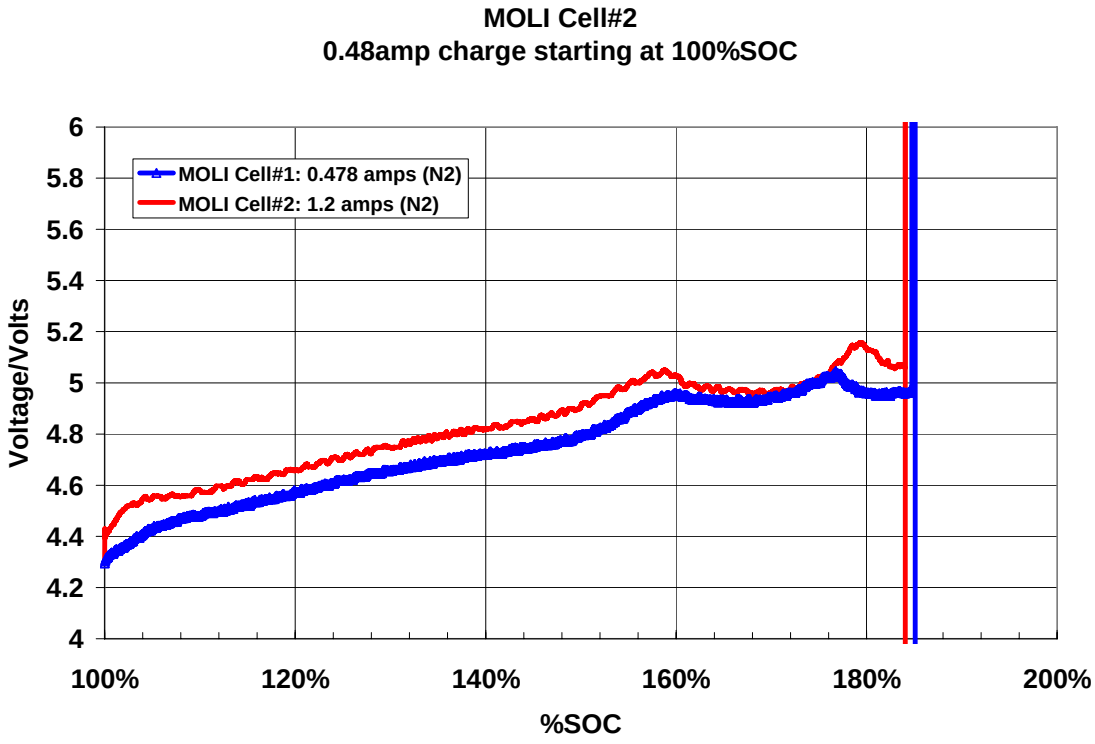

Figure 24. Overcharge cell voltage profiles for Moli cells at C/5 and C/2 charge rates.

2.5 Thermal Runaway (ARC)

Thermal runaway response of the cells was measured in the accelerating rate calorimeter (ARC) under adiabatic conditions up to 450°C at increasing states of charge (3.8V, 4.0V, 4.2V, 4.3V). Thermal runaway is defined as the self-generated heating of the cell which exceeds a threshold rate limit of 0.02°C /min under the ARC adiabatic conditions. A new fixture was designed and constructed to allow full thermal runaway of the 18650 cells in a sealed container which minimized the expansion volume for the evolved gases. This low volume reduced cooling of the cells during the high gas release thermal runaway but also significantly increased the pressure in the cell fixture. These controlled conditions allow a better side-by-side comparison of the different commercial cells. However, a thermal runaway/vent reaction into an unconstrained volume would have somewhat reduced heating rates. The gas pressure during the run was measured and used to calculate the STP equivalent volume of generated gas. Most of the runs maintained a pressure seal up to 2000psi at 500°C but some of the runs experienced a pressure leak during the explosive runaway. The pressure data after a leak event was not used to calculate evolved gas volumes and is indicated by a truncated display in the figures.

Figure 25 shows the heating rate data for the four MOLI cells at increasing voltages. Heating rates were measured as high as 1200°C/min. At heating rates higher than about 10°C /min the cell temperature exceeds the ability of the ARC to maintain adiabatic conditions and the cell temperature will temporarily exceed the ARC temperature. After the thermal runaway peak the cell temperature will cool back down to the ARC temperature and the controlled run will continue. Usually, the maximum ARC temperature has been reached and the ARC begins active cooling. The high cell heating rates began in the range 180°C - 200°C, increasing with increasing cell voltage. Peak heating rates occurred in the range of 250°C - 300°C. The onset of thermal runaway is more clearly shown in Figure 26. Onset occurred around 160°C for the 3.8V cell and decreased with increasing cell voltage down to 130°C for the 4.3V cell.

Measured gas evolution was detected after cell venting which typically occurred in the 130°C - 150°C range (Figure 27). The temperature of cell venting decreased with increasing cell voltage indicating that higher states of charge result in increased gas generation in the cell leading to higher internal pressures. The 3.8V cell did not show a discrete vent but showed increased gas generation starting at 120°C, suggesting that it may have had a leaky seal. After venting, all of the cells showed similar gas evolution rates with increasing temperature up to the thermal runaway temperature with a total evolved gas level of 300ml – 350ml just prior to runaway. During thermal runaway the evolved gases did not increase at the same rapid rate as the temperature. However, the gas volume increased steadily over time even while the cell was cooling (Figure 28). The total gas volume evolved for these Moli cells in this “smoking rubble” state was about 1700 ml (+/- 200 ml). There was some larger volume of gas associated with the higher cell voltages.

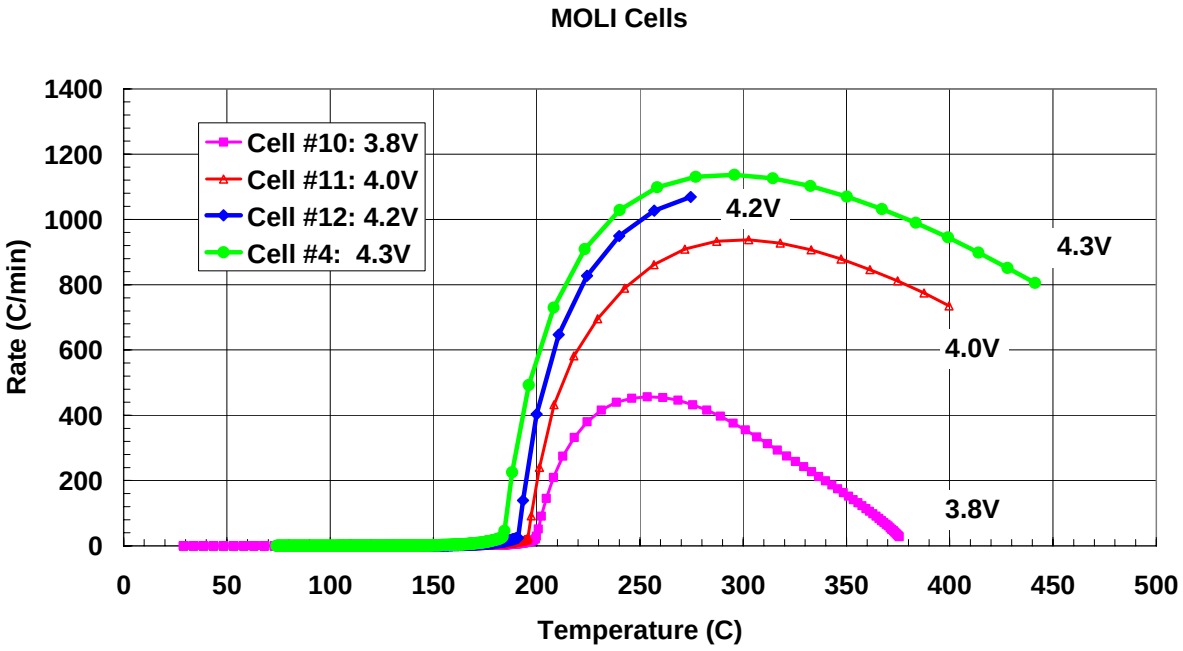

Figure 25. ARC thermal runaway profile for Moli cells at increasing SOC.

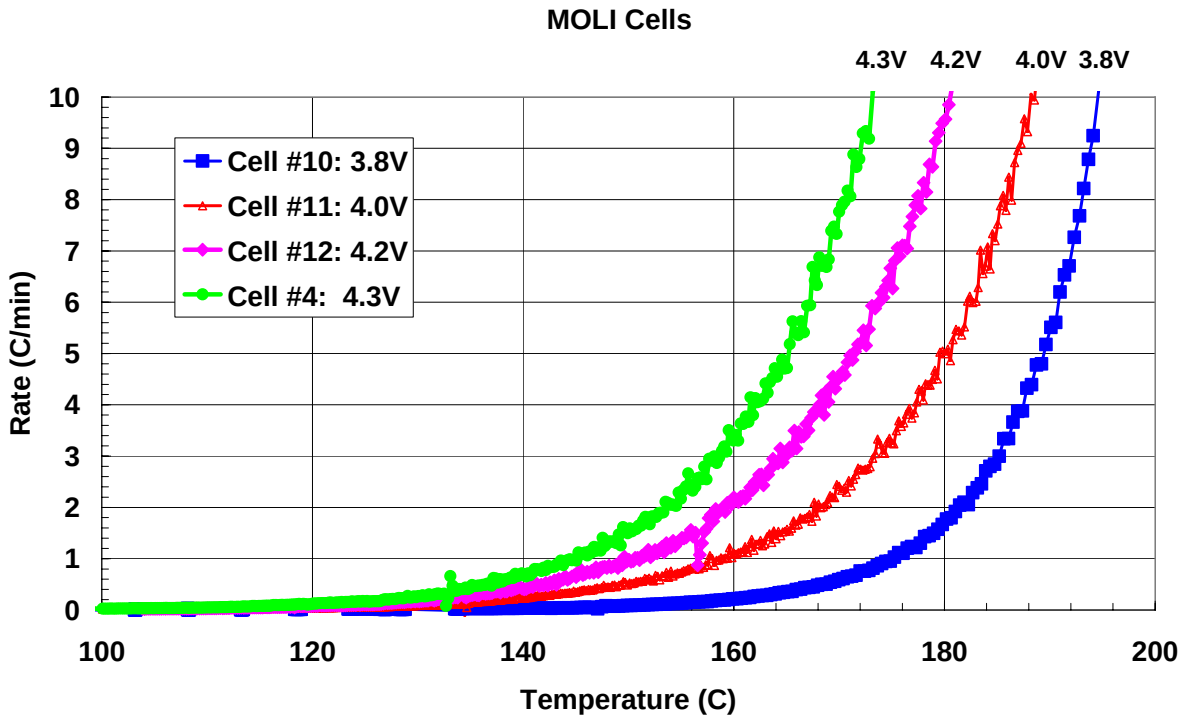

Figure 26. Onset of thermal runaway for Moli cells at increasing SOC.

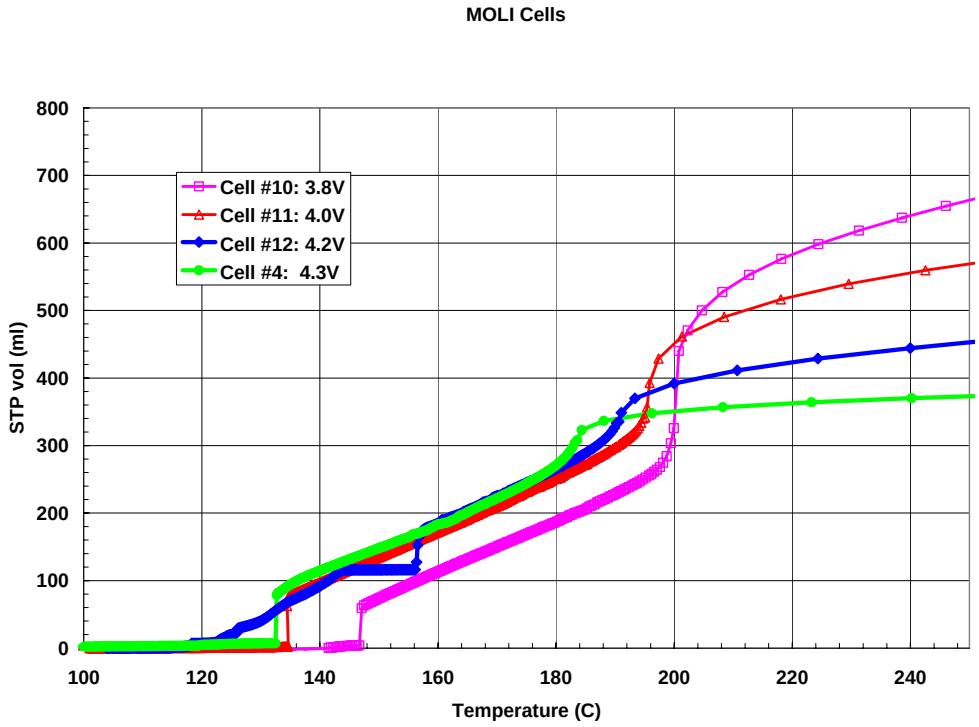

Figure 27. Gas generation during ARC runs of Moli cells up to thermal runaway temperatures.

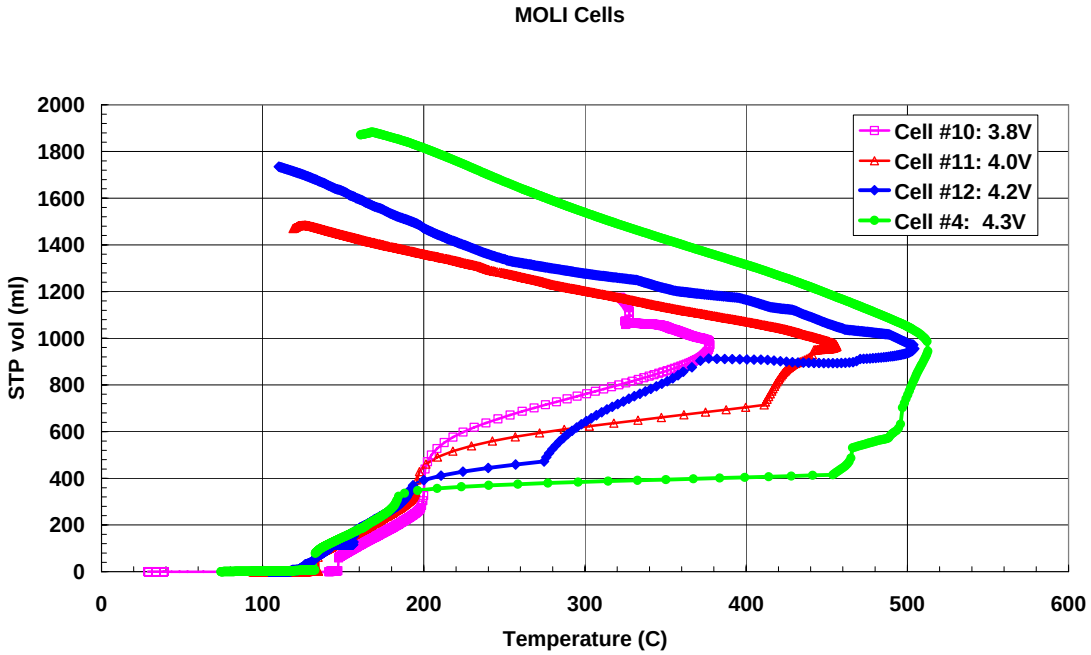

Figure 28. Gas generation during ARC runs of Moli cells during thermal runaway and cooling.

3.0 Panasonic Cells

3.1 Electrical Acceptance Test

Five Panasonic cell were received for evaluation of thermal runaway performance only. The initial acceptance data is shown in Table 6. All cells appeared normal. Electrical acceptance tests were performed as described for the Moli cells except that the pulse loading tests were performed at 100%SOC potential of 4.2V. Two charge/discharge cycles were performed at a C/3 rate giving an average cell capacity of 2.14 Ah. A 1.5C, 30s load pulse was then applied to each cell starting at the 100%SOC voltage of 4.2V. Table 7 lists the results for each of the five cells. An ohmic impedance of 103 mohms was measured with an average final cell resistance of 127 mohms (compared to 161 mohms for the Moli cells). A typical load pulse profile is shown in Figure 29.

Table 6. Incoming Inspection Values for Panasonic Cells

NASA Panasonic cells				
#	Weight(g)	Height (mm)	Diameter (mm)	OCV
NP228	42.94	64.9	18.1	3.363
NP229	43.23	64.8	18.1	3.367
NP230	43.17	65.1	18.1	3.365
NP231	43.35	64.8	18.2	3.366
NP232	43.03	64.8	18.2	3.356
Average	**43.15**	**64.88**	**18.13**	**3.363**
StdDev	0.16	0.13	0.07	0.004

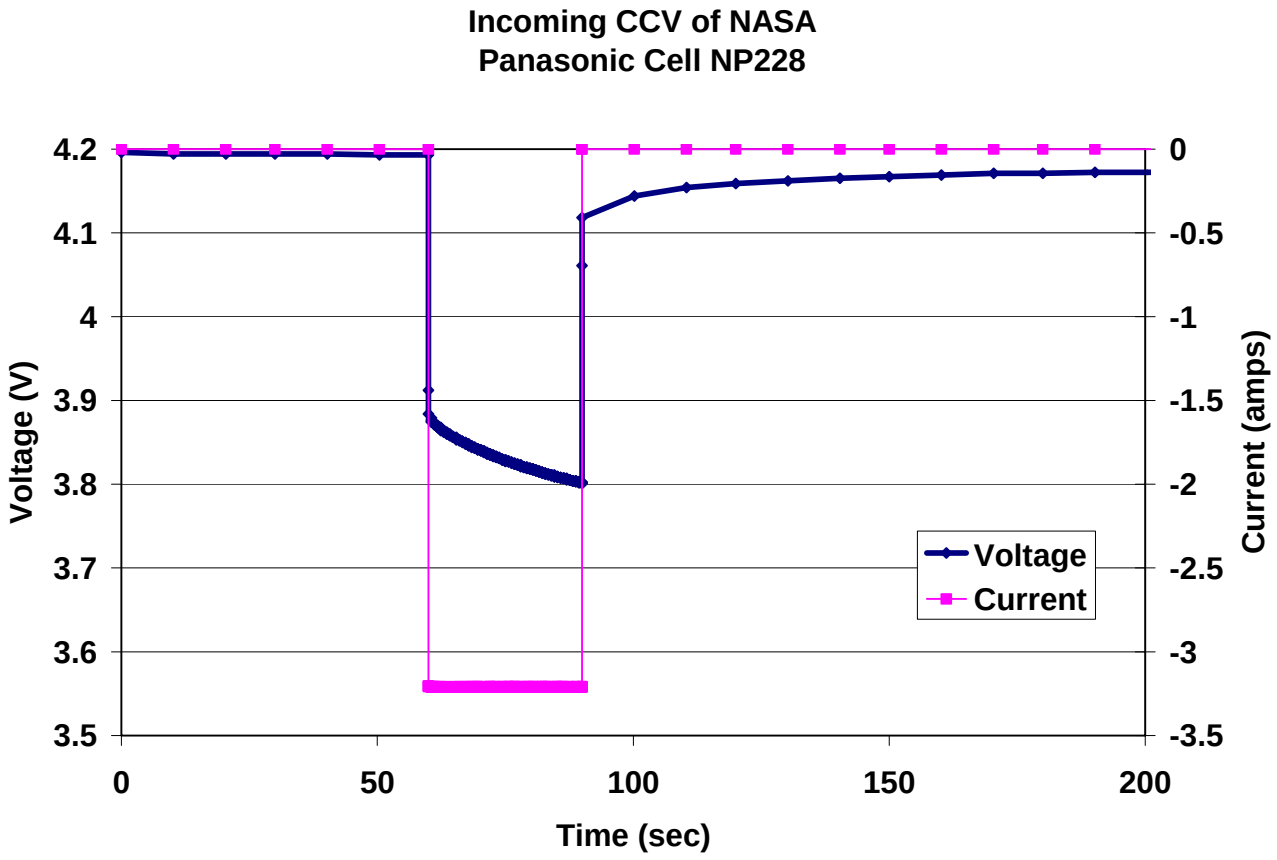

Figure 29. Typical load profile of Panasonic cell during 1.5C/30s load.

Table 7. Electrical Acceptance Tests for Panasonic Cells

Cell	Discharge Capacity1 (Ah)	Discharge Capacity2 (Ah)	Vo	V1	V2	Ohmic Res. (V0-V1)/I	Final Res. (Vo-V2)/I	Diff.
NP228	2.139	2.135	4.193	3.884	3.801	0.096	0.122	0.026
NP229	2.143	2.14	4.193	3.879	3.806	0.098	0.121	0.023
NP230	2.139	2.136	4.192	3.816	3.739	0.117	0.141	0.024
NP231	2.147	2.143	4.193	3.866	3.784	0.102	0.127	0.026
NP232	2.148	2.144	4.194	3.868	3.803	0.102	0.122	0.020
Avg=	**2.143**	**2.140**			**Avg=**	**0.103**	**0.127**	**0.024**
Std. Dev.=	0.004	0.004			Std. Dev.=	0.008	0.009	0.002

3.2 ARC Thermal Runaway

The Panasonic cells were also measured in the ARC from 3.8V to 4.3V. High rate thermal runaway was again observed in the 180°C to 200°C range as seen for the Moli cells. Peak heating rates were also seen up 1200°C/min as shown in Figure 30. Expansion of the onset temperature regime shows similar responses as seen for the Moli cells (Figure 31). Thermal runaway onset temperature decreased and heating rates increased with increasing cell voltage. All of the cells showed discrete vents with venting temperatures decreasing from 145°C to 120°C with increasing cell voltage (Figure 32). Gas evolution rates were similar after venting up to thermal runaway and each cell resulted in about 250ml – 300 ml of gas prior to runaway. Total evolved gas after runaway and subsequent cooling increased with increasing voltage up to a maximum of 2400 ml for the 4.2V cell (Figure 33). The 4.3V developed a leak at the thermal runaway event and gas volume was not recorded.

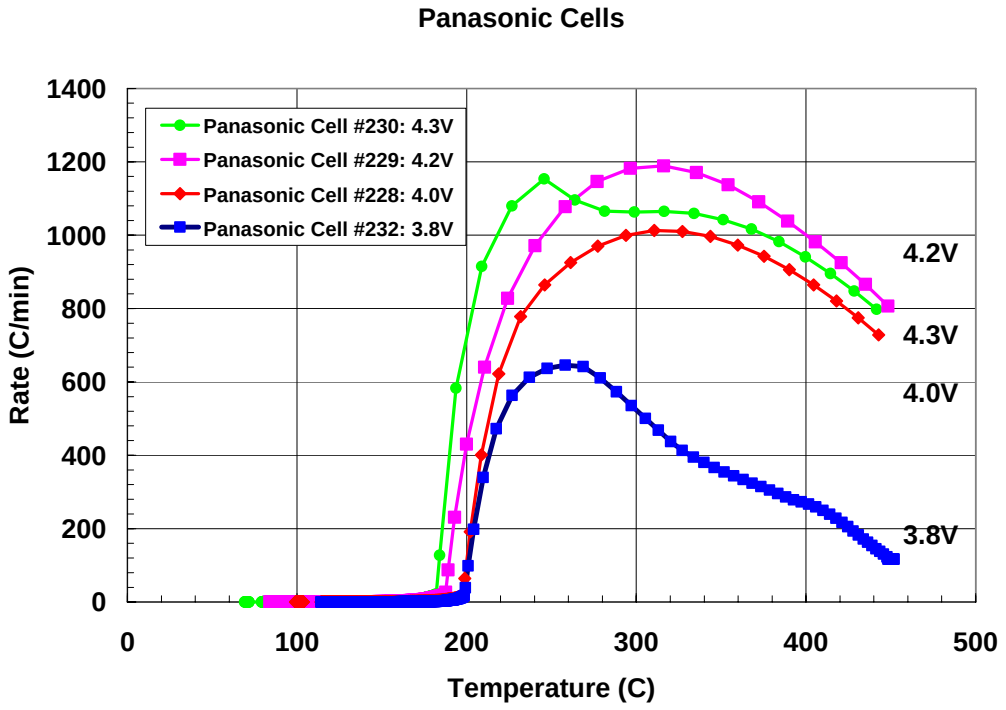

Figure 30. ARC thermal runaway profile for Panasonic cells at increasing SOC.

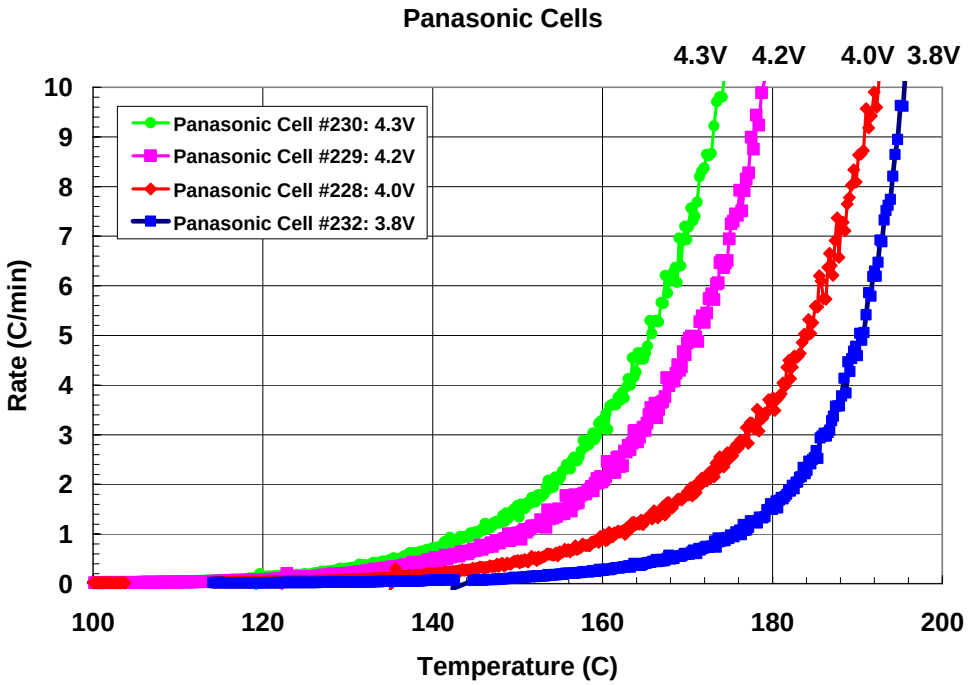

Figure 31. Onset of thermal runaway for Panasonic cells at increasing SOC.

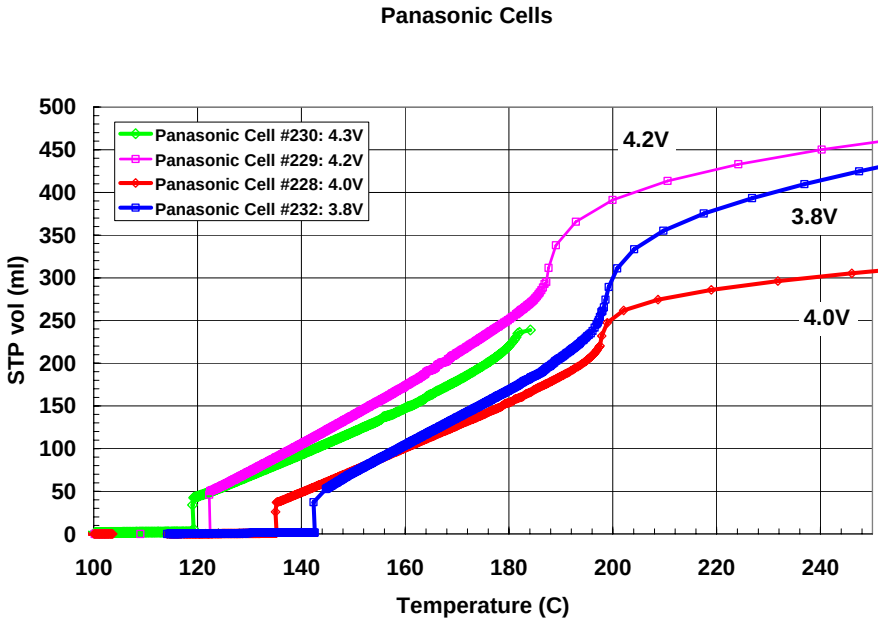

Figure 32. Gas generation during ARC runs of Panasonic cells up to thermal runaway temperatures.

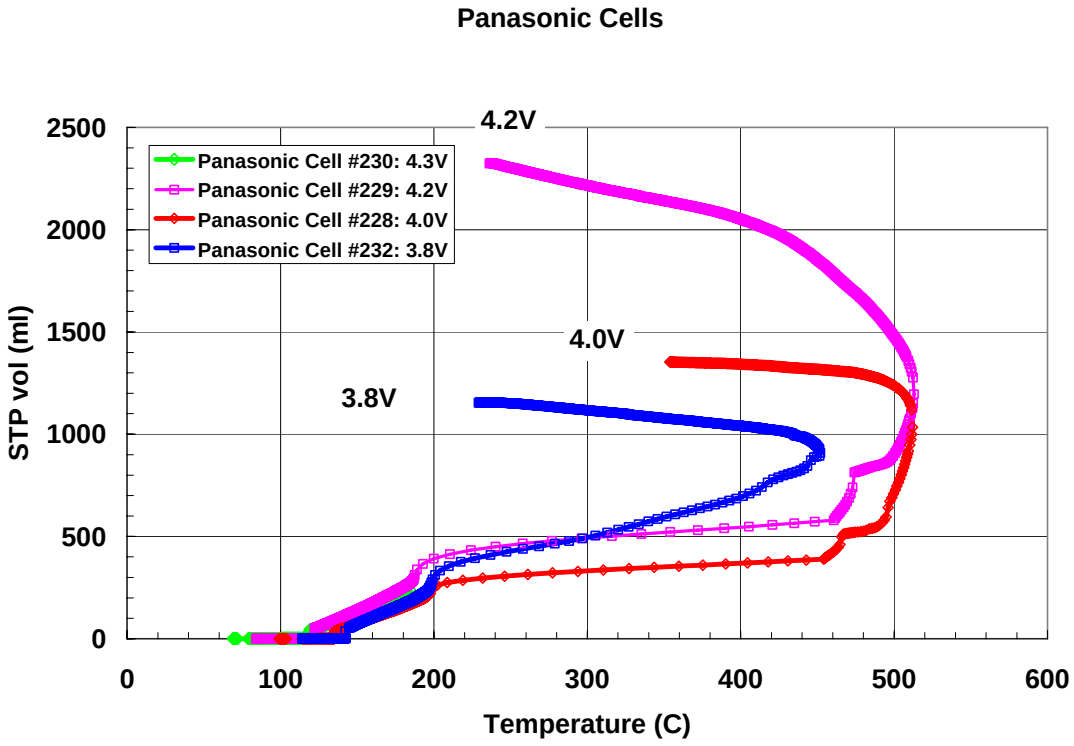

Figure 33. Gas generation during ARC runs of Panasonic cells during thermal runaway and cooling.

4.0 Sanyo Cells

4.1 Electrical Acceptance Test

Five Sanyo cell were received for evaluation of thermal runaway performance only. The initial acceptance data is shown in Table 8. All cells appeared normal. Electrical acceptance tests were performed as described for the other cells. Two charge/discharge cycles were performed and a 1.5C, 30s load pulse was applied to each cell with the cells at 4.2V. Table 9 lists the results for each of the five cells. The average cell capacity was 2.14 Ah (same as for the Panasonic cells) and the average final cell resistance was 152 mohms (126 mohms ohmic), slightly higher than for the Panasonic cells (127 mohms total/103 mohms ohmic). The pulse load tests were performed at 4.2V as was done for the Panasonic cells. A typical load pulse profile is shown in Figure 34. Two of the cells showed an irregular voltage profile for a few seconds after pulse loading but the profiles stabilized after a few seconds. The other cells showed profiles similar to the other two commercial cells.

Table 8. Incoming Inspection Values for Sanyo Cells

NASA Sanyo cells				
#	Weight(g)	Height (mm)	Diameter(mm)	OCV
NS772	45.30	64.8	18.1	3.788
NS788	45.27	65.1	18.2	3.788
NS809	45.12	64.8	18.1	3.788
NS829	45.63	64.8	18.1	3.788
NS830	45.33	64.9	18.2	3.788
Average	**45.33**	**64.89**	**18.15**	**3.788**
StdDev	0.19	0.13	0.02	0.000

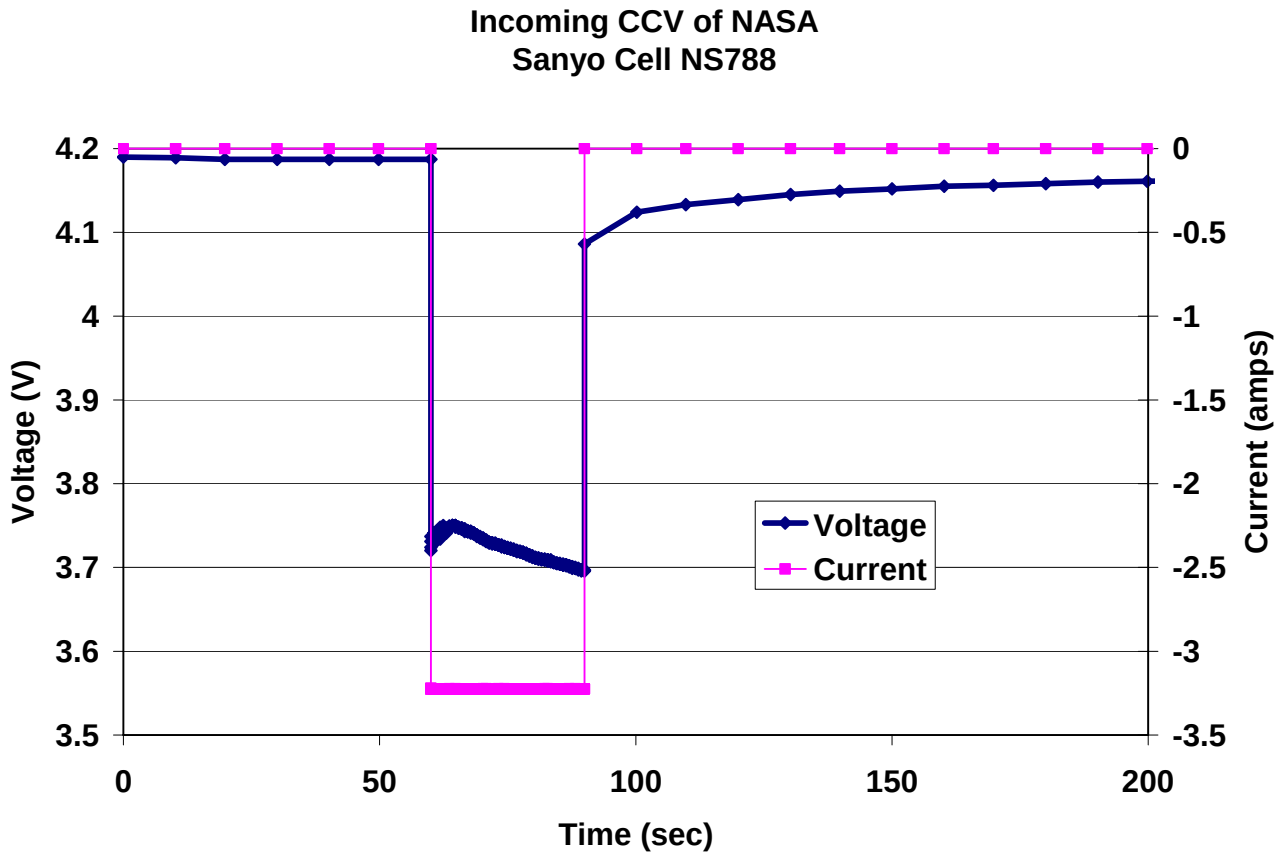

Figure 34. Typical load profile of Sanyo cell during 1.5C/30s load.

Table 9. Acceptance Tests for Sanyo Cells

Cell	Discharge Capacity1 (Ah)	Discharge Capacity2 (Ah)	Vo	V1	V2	Ohmic Res. (V0-V1)/I	Final Res. (Vo-V2)/I	Diff.
NS772	2.138	2.134	4.191	3.712	3.644	0.149	0.170	0.021
NS788	2.141	2.142	4.187	3.738	3.696	0.139	0.152	0.013
NS809	2.127	2.125	4.192	3.805	3.744	0.120	0.139	0.019
NS829	2.152	2.152	4.192	3.859	3.779	0.103	0.128	0.025
NS830	2.147	2.146	4.192	3.801	3.642	0.121	0.171	0.049
Avg=	**2.141**	**2.140**			**Avg=**	**0.126**	**0.152**	**0.025**
Std. Dev.=	0.010	0.011			Std. Dev.=	0.018	0.019	0.014

4.2 ARC Thermal Runaway

The Sanyo cells were also measured in the ARC from 3.8V to 4.3V. High rate thermal runaway was again observed in the 180°C to 200°C range as seen for the Moli and Panasonic cells. Peak heating rates were seen up 900°C/min as shown in Figure 35, lower than seen for the other cells. Expansion of the onset temperature regime shows similar responses as seen for the Moli and Panasonic cells but with two additional reaction events seen for the 4.0V and 4.3V cells (Figure 36). These reactions could result from interactions with electrolyte additives for this particular cell chemistry. Thermal runaway onset temperature decreased and heating rates increased with increasing cell voltage as seen for the other cells. All of the cells showed discrete vents over a narrow range (125°C to 130°C) with venting temperatures slightly decreasing with increasing cell voltage (Figure 37). Gas evolution rates were similar after venting up to thermal runaway and each cell resulted in about 350 ml of gas prior to runaway (the 3.8V and 4.3V cells developed leaks). Total evolved gas after runaway and subsequent cooling increased with increasing voltage up to a maximum of 2400 ml for the 4.2V cell (Figure 38).

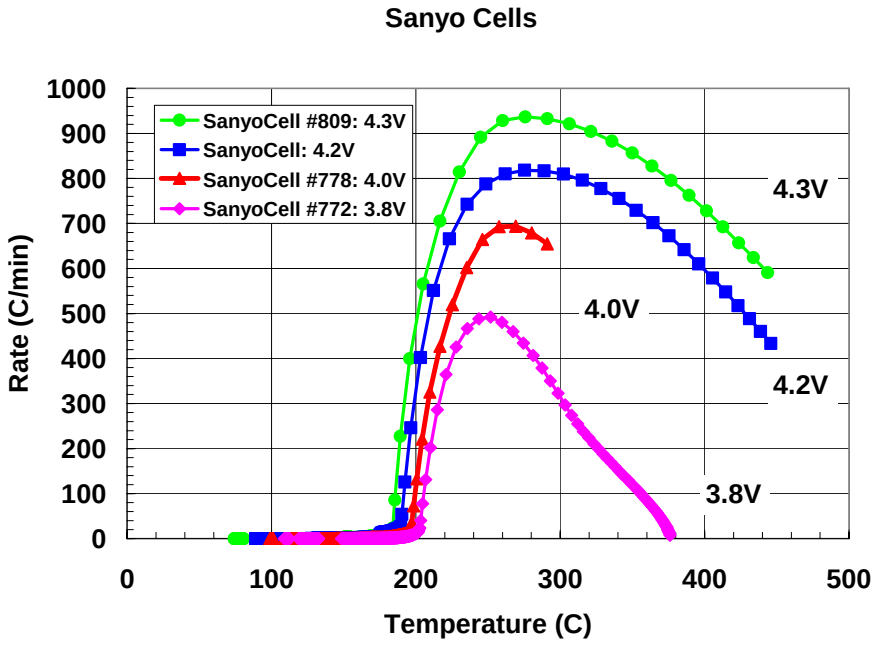

Figure 35. ARC thermal runaway profile for Sanyo cells at increasing SOC.

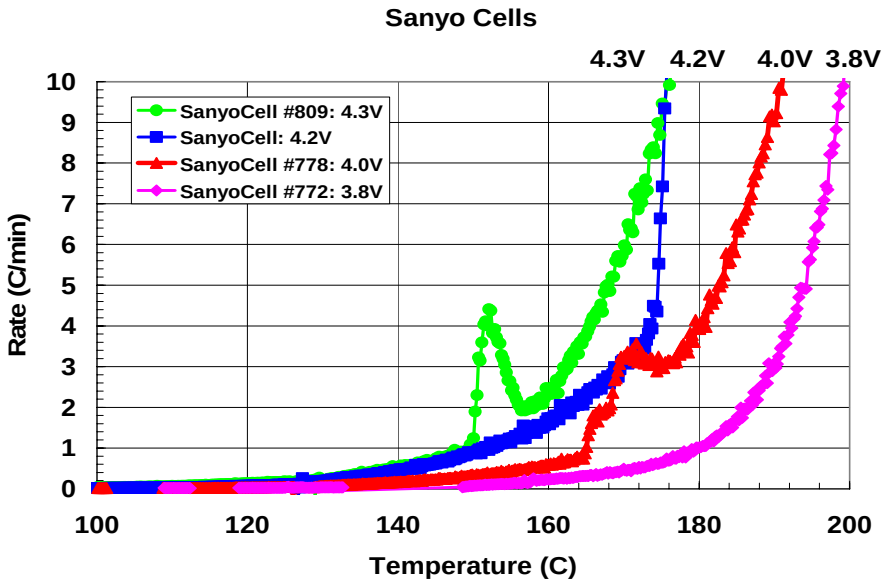

Figure 36. Onset of thermal runaway for Panasonic cells at increasing SOC.

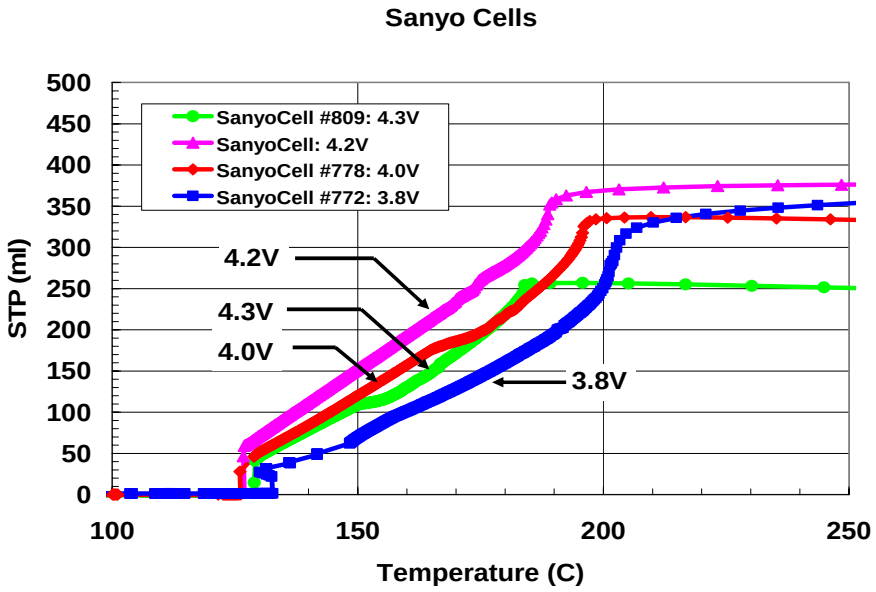

Figure 37. Gas generation during ARC runs of Sanyo cells up to thermal runaway temperatures.

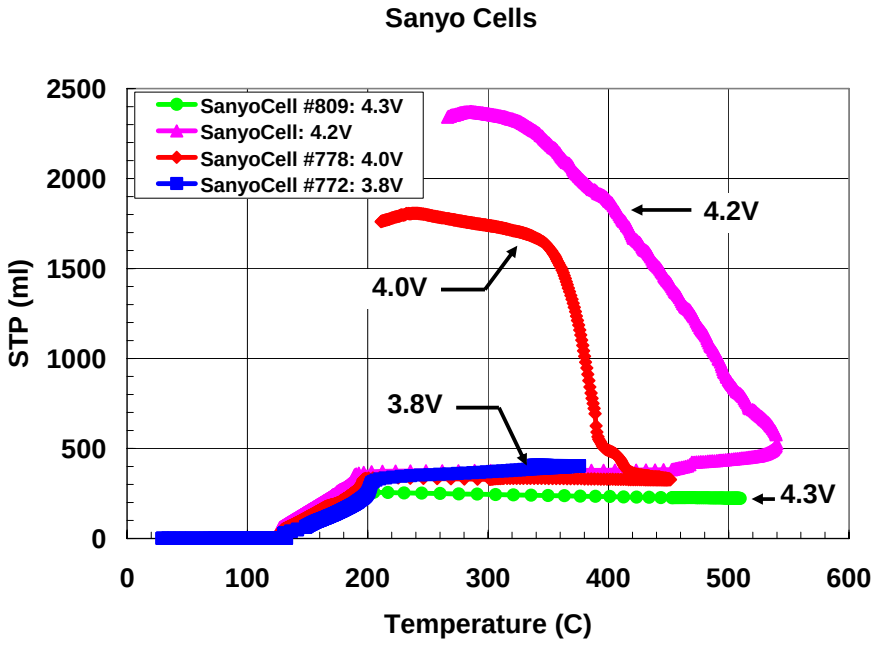

Figure 38. Gas generation during ARC runs of Sanyo cells during thermal runaway and cooling.

5.0 Cell Comparisons

These measurements of the Moli, Panasonic and Sanyo cells described in this report were preceded by an earlier series of measurements of commercial Sony cells (1.4 A/h). The ARC thermal runaway response for these cells was measured at cell voltages of 4.1V, 4.2V, 4.3V, 4.4V and 4.5V. These cells were measured using an early cell fixture which did not allow pressure controlled measurements above the peak thermal runaway temperature and the relative ARC data only shows runaway up to the 150°C -200°C range. Comparisons of the current cells with the Sony cells are made at the same (or similar) cell voltages. The ARC thermal runaway profiles at each cell voltage are compared in Figures 39 – 52. Comparisons are also made with the Sony cells measured in an earlier study for some of the cell voltages.

- **3.8V** (Figures 39 and 40): The thermal runaway onsets are very similar (150°C) but the Sanyo cell showed slightly lower heating rate. The Panasonic cell showed somewhat higher peak heating rate of 650°C/min at 275°C.

- **4.0V** (Figures 41 and 42): The Sanyo cell showed a definite lower peak heating rate (700°C/min) than for either the Panasonic or Moli cells. The onset temperature profiles all looked the same with an onset temperature around 140°C. The peak heating rates increased up to 1000 °C/min and continued up to 300°C. Figures 43 and 44 show the same data compared with the Sony data. The Sony cells showed higher heat output at low temperatures with an untypical exothermic reaction between 135°C - 175°C and then showing lower reaction rate at higher temperatures. The Sony cells were not measured under controlled conditions through the runaway peak and the data are not shown.

- **4.2V** (Figure 45 and 46): The Sanyo cell showed much lower peak heating rate (800°C/min) compared to the Moli and Panasonic cells which were both very similar at 1200°C/min. The onset temperature profiles were very similar starting at 130°C. Peak heating rates remained around 300°C. The Sony cell comparisons are shown in Figures 47 and 48. The Sony cell again showed increased heat out at the low temperatures. A distinctive breakdown of the anode protective layer is seen at 110°C followed by an exothermic reaction between 135°C and 165°C. At higher temperatures the heating rates were similar to the other cells.

- **4.3V** (Figure 49 and 50): The Sanyo cell still shows a lower peak heating rate (900°C/min) but is much closer to the Moli and Panasonic cells (1100°C/min). The onset temperatures are still similar with onset around 120°C. The Sanyo cell showed the narrow reaction peak around 150°C. Peak heating rates remained

around 300°C. The Sony cell comparison is shown in Figures 51 and 52. The breakdown of the anode layer was again seen at 110°C but no reaction peak was seen at 135°C. At 4.2V, the Sony cells and the three commercial cells studied here behaved very similarly.

Overall, the Sanyo cells show slightly better thermal runaway performance but have lower capacity than the Moli cells. The Sanyo cells show some evidence of additives or electrode stabilization but these do not have any significant detrimental effect on cell thermal performance. The Moli cells had similar thermal response to the Panasonic cells but with increased capacity. For the same capacity level, the Sanyo cells showed superior thermal performance over the Panasonic cells. Table 10 shows a comparison of the thermal and electrical data obtained for each of the three current commercial cells and the previous Sony cells.

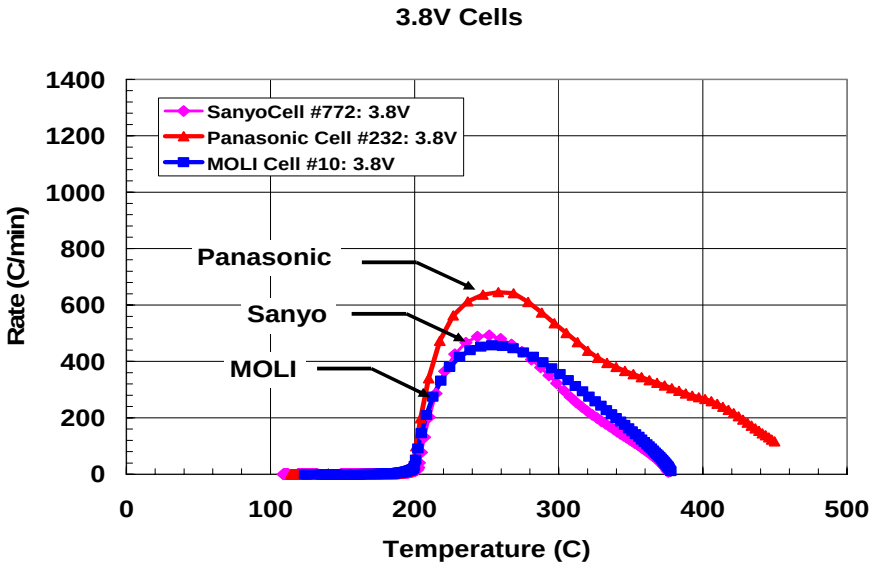

Figure 39. ARC comparison of all three commercial cells during thermal runaway at 3.8V.

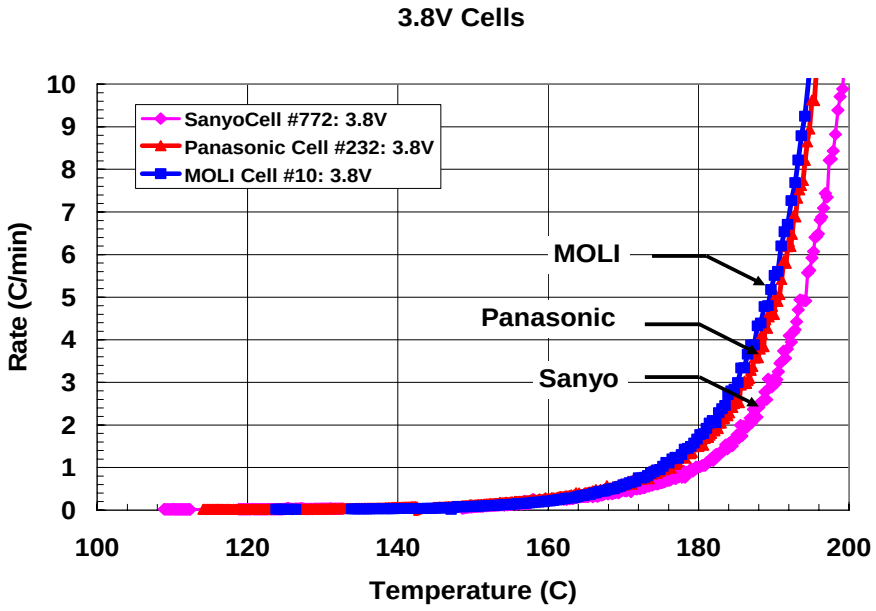

Figure 40. Comparison of onset of ARC thermal runaway for all three commercial cells at 3.8V.

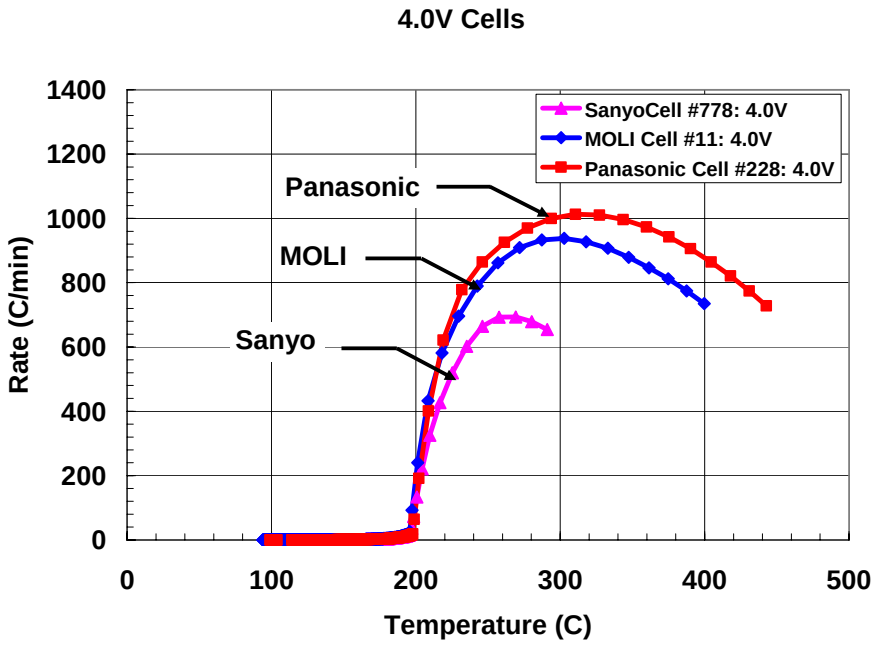

Figure 41. ARC comparison of all three commercial cells during thermal runaway at 4.0V.

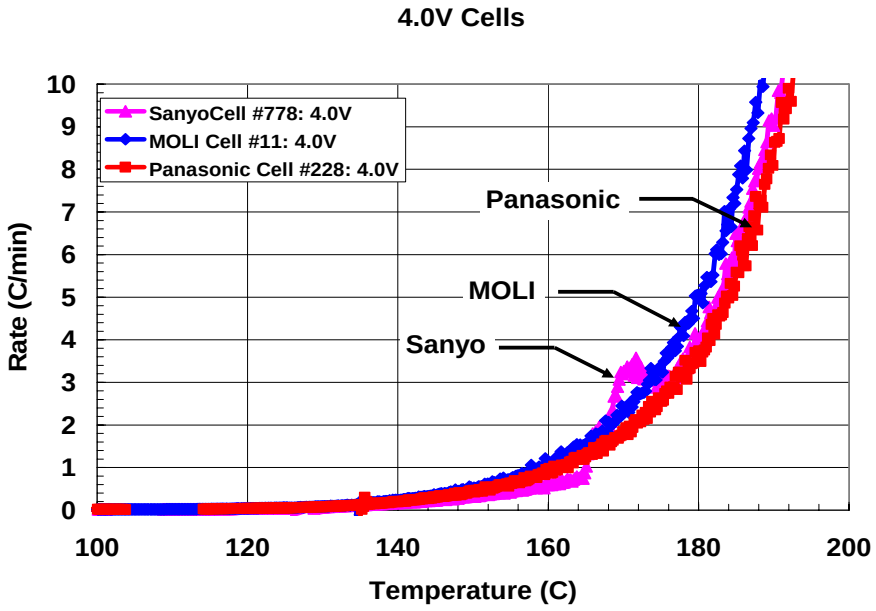

Figure 42. Comparison of onset of ARC thermal runaway for all three commercial cells at 4.0V.

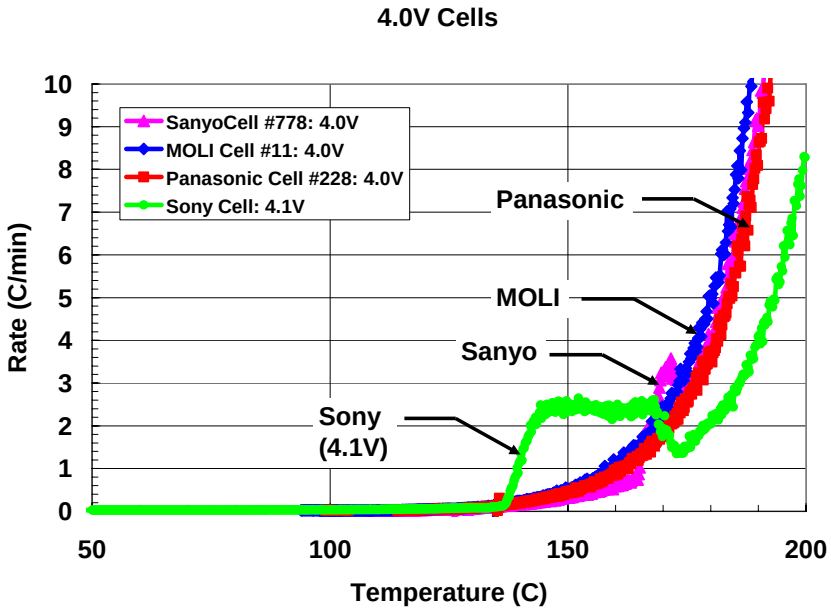

Figure 43. Comparison of onset of ARC thermal runaway for all three commercial cells at 4.0V and the earlier Sony cells at 4.1V.

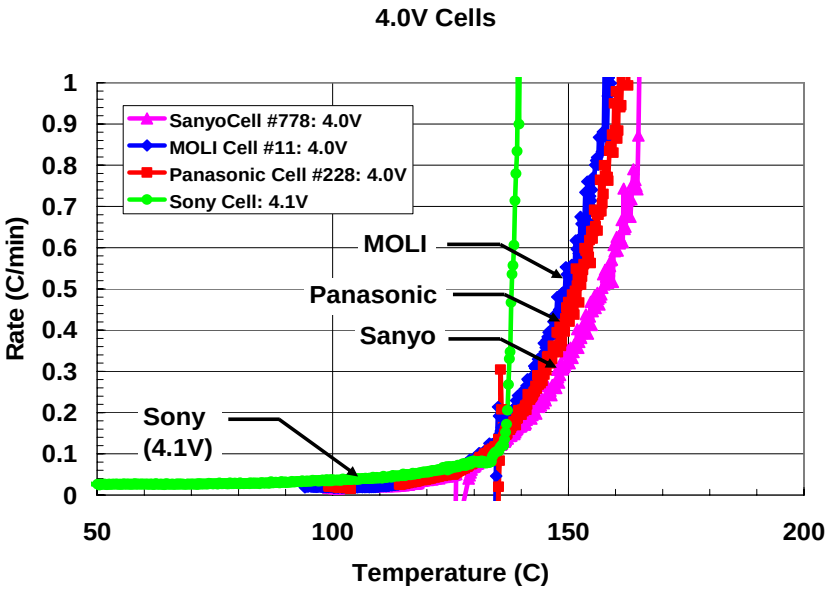

Figure 44. Comparison of onset of ARC thermal runaway for all three commercial cells at 4.0V and the earlier Sony cells at 4.1V (expanded scale).

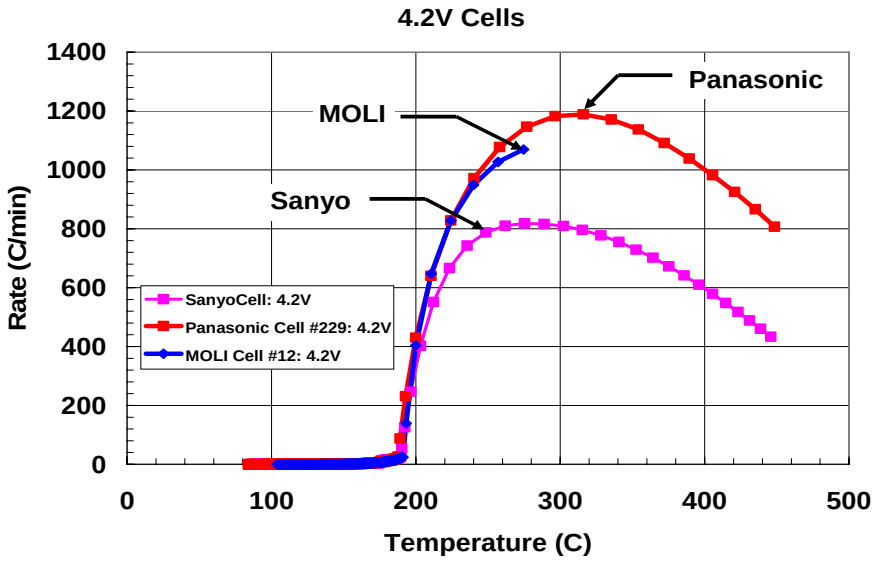

Figure 45. ARC comparison of all three commercial cells during thermal runaway at 4.2V.

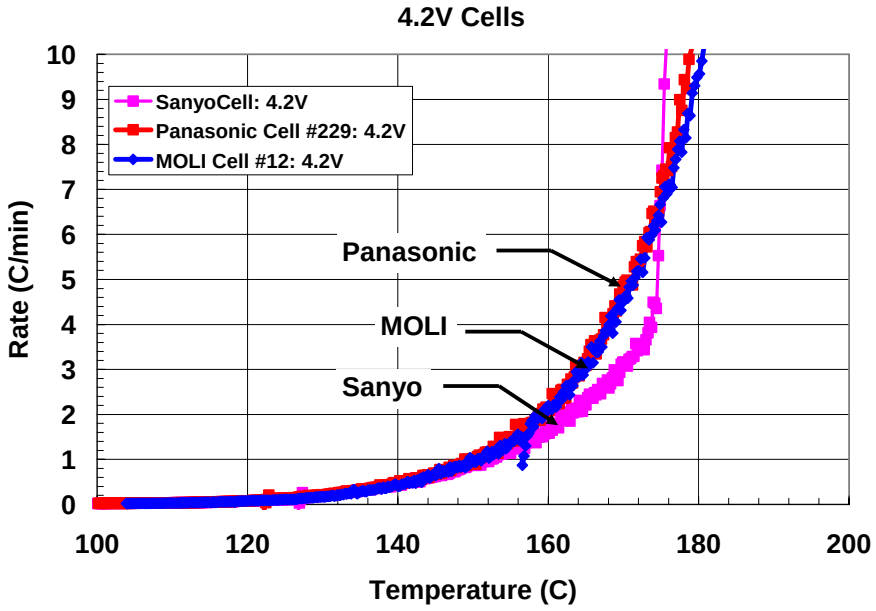

Figure 46. Comparison of onset of ARC thermal runaway for all three commercial cells at 4.2V.

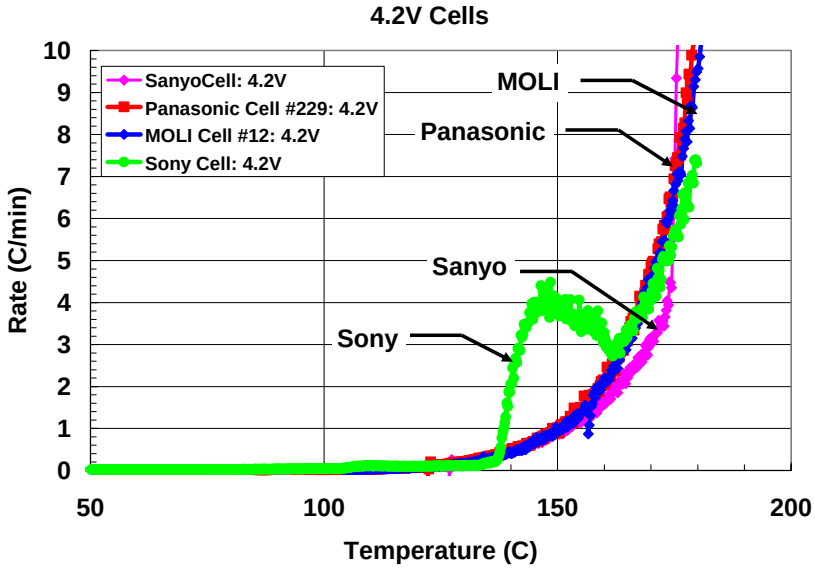

Figure 47. Comparison of onset of ARC thermal runaway for all three commercial cells and the earlier Sony cells at 4.2V.

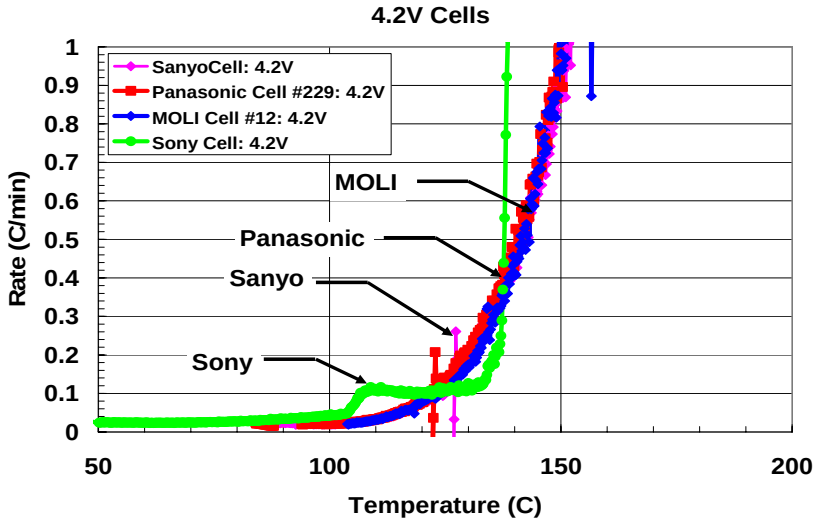

Figure 48. Comparison of onset of ARC thermal runaway for all three commercial cells and the earlier Sony cells at 4.2V (expanded scale).

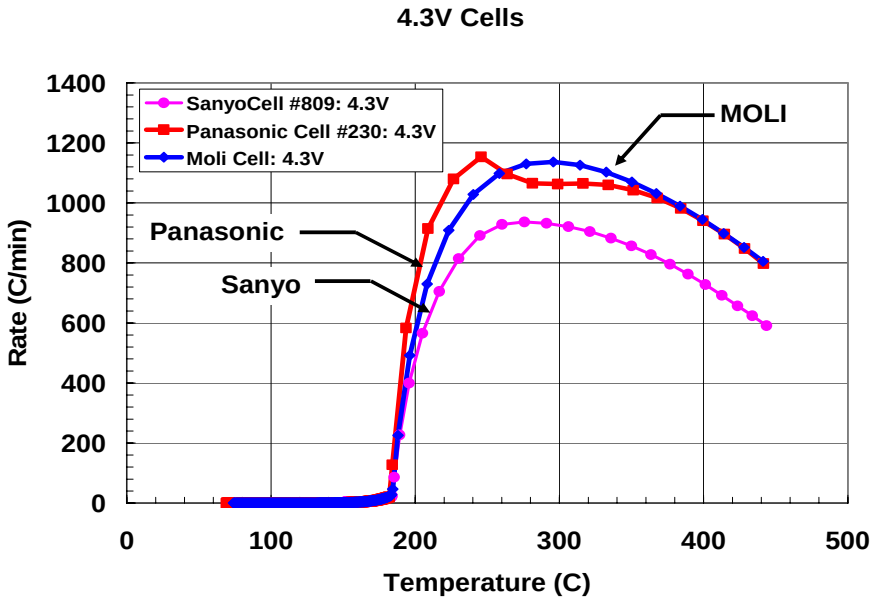

Figure 49. ARC comparison of all three commercial cells during thermal runaway at 4.3V.

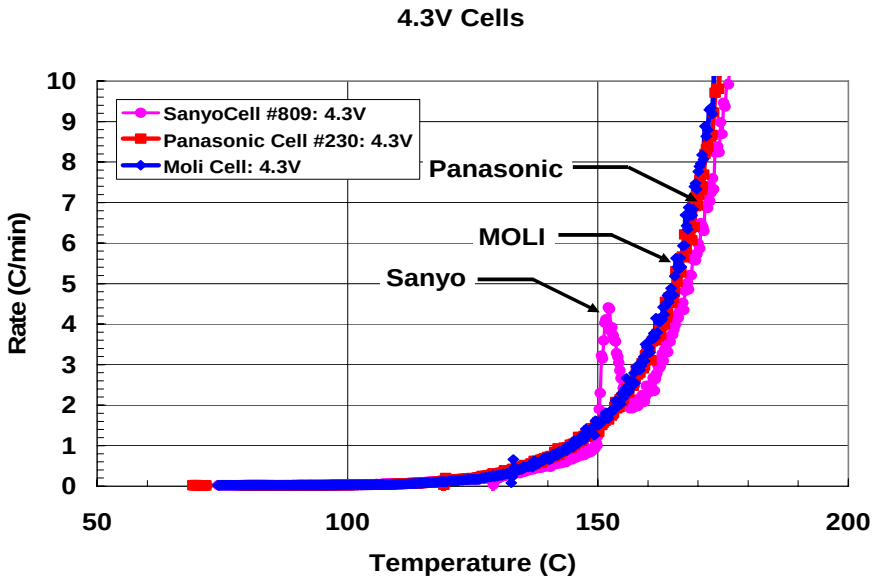

Figure 50. Comparison of onset of ARC thermal runaway for all three commercial cells at 4.3V.

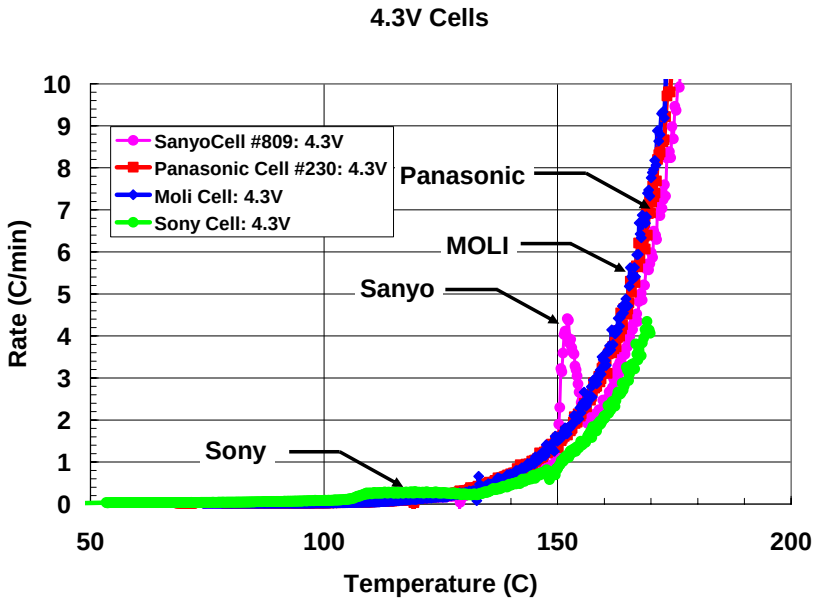

Figure 51. Comparison of onset of ARC thermal runaway for all three commercial cells and the earlier Sony cells at 4.3V.

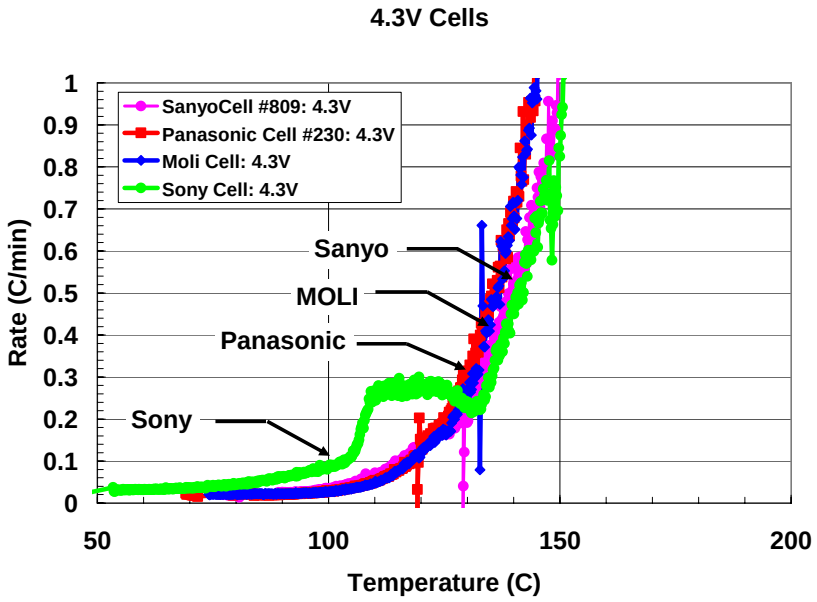

Figure 52. Comparison of onset of ARC thermal runaway for all three commercial cells and the earlier Sony cells at 4.3V (expanded scale).

Table 10. Comparison of Commercial 18650 Li-Ion Cells

Parameter	Sony	Moli	Panasonic	Sanyo
Weight (grams)	40.92	47.60	43.15	45.33
Discharge Capacity (C/2 or less)	1.39 Ah (0.75 amp)	2.30 Ah (0.5 amp)	2.14 Ah (0.75 amp)	2.14 Ah (0.5 amp)
30s Load DC Resistance Ohmic/Total (ohms)	0.116/0.124 (1.5C/2.25 A) (4.2V OCV)	0.117 / 0.161 (1C/2.25 A) (3.8V OCV)	0.103 / 0.127 (1.5C/3.2 A) (4.2V OCV)	0.126 / 0.152 (1.5C/3.2 A) (4.2V OCV)
Heat Capacity (J/g-C)	0.902	0.823	na	na
MicroCal Heat (55 C and 4.2 V)	1125 uW	1676 uW	na	na
MicroCal Heat (55 C and 3.8 V	377 uW	515 uW	na	
MicroCal Heat (35 C and 4.2 V)	345 uW	509 uW	na	na
MicroCal Heat (35 C and 3.8 V	142 uW	102 uW	na	na
Self Discharge Activation Energy	53.5 kJ/mole@ 3.8V 41.3 kJ/mole@ 4.0V 49.6 kJ/mole@ 4.2V	65.4 kJ/mole@ 3.8V 57.6 kJ/mole@ 4.0V 51.2 kJ/mole@ 4.2V	na	na
ARC Onset of Thermal Runaway (>0.02C/min)	70 C @ 4.1V 60 C @ 4.2V 55 C @ 4.3V 40 C @ 4.4V 40 C @ 4.5V	125 C @ 3.8V 110 C @ 4.0V 105 C @ 4.2V 75 C @ 4.3V	120 C @ 3.8V 114 C @ 4.0V 94 C @ 4.2V 80 C @ 4.3V	119 C @ 3.8V 109 C @ 4.0V 100 C @ 4.2V 90 C @ 4.3 V
ARC High Rate Thermal		195 C @ 3.8V	195 C @ 3.8V	200 C @ 3.8V

Runaway (>10C/min)	**200 C @ 4.1V** **180 C @ 4.2V** **170 C @ 4.3V** **170 C @ 4.4V** **190 C @ 4.5V**	**188 C @ 4.0V** **180 C @ 4.2V** **173 C @ 4.3V**	**192 C @ 4.0V** **179 C @ 4.2V** **174 C @ 4.3V**	**191 C @ 4.0V** **176 C @ 4.2V** **176 C @ 4.3V**
ARC Peak Heating Rate Temperature	**Cells cooled before peak runaway**	**254 C @ 3.8V** **303 C @ 4.0V** **275 C @ 4.2V** **296 C @ 4.3V**	**258 C @ 3.8V** **310 C @ 4.0V** **316 C @ 4.2V** **leak @ 4.3V**	**252 C @ 3.8V** **269 C @ 4.0V** **275 C @ 4.2V** **275 C @ 4.3V**
ARC Peak Heating Rate	**Cells cooled before peak runaway**	**457 C/min @ 3.8V** **934 C/min @ 4.0V** **1071C/min @ 4.2V** **1136C/min @ 4.3V**	**645C/min @ 3.8V** **1013C/min@4.0V** **1189C/min@4.2V** **leak @ 4.3V**	**492 C/min@ 3.8V** **694 C/min@4.0V** **818 C/min@4.2V** **937 C/min@ 4.3V**

6.0 Distribution

Brad Irlbeck
NASA
Lyndon B. Johnson Space Center
Mail Code: EP5
Houston, TX 77058

Dr. Eric C. Darcy
NASA
Lyndon B. Johnson Space Center
Energy Systems Division MS: EP5
Houston, TX 77058

Spencer Watson
Department of Transportation
400 7th Street
Room 8436C
Washington, DC 20590

MS-0521	Michael R. Prairie (2520)
MS-0613	Daniel H. Doughty (2521)
MS-0613	E. Peter Roth (2521) (10)
MS-0613	David Johnson (2521)
MS-9018	Central Technical Files (8945-1)
MS0899	Technical Library, (9616) (2)